e-ISSN: 3061-9939

JOURNAL OF NAVAL ARCHITECTURE AND MARINE TECHNOLOGY

ISSUE 228, 2026

www.jnamt.org

RESEARCH ARTICLE

DOI: 10.54926/jnamt.2025.2526

J Nav Architect Mar Technol 2026;228:1-10

Microplastic Pollution in Ship-Sourced Wastewater: Assessment of Pollution Load Risk for Ballast and Bilge Water

Emrah Şık

İstanbul Technical University Faculty of Maritime, Department of Basic Sciences, İstanbul, Türkiye

To cite this article: E. Şık. Microplastic pollution in ship-sourced wastewater: assessment of pollution load risk for ballast and bilge water. *J Nav Architect Mar Technol*. 2026;228:1-10

Received: 08.09.2025 - **Revision Requested:** 02.11.2025 - **Last Revision Received:** 07.11.2025 - **Accepted:** 01.12.2025 - **Publication Date:** 07.01.2026

Abstract

The rapid development of maritime transport also causes a number of negative environmental impacts. One of these problems is marine pollution caused by the operation of ships. Pollution from ship sewage includes ballast water (BAL-W) and bilge water (BIL-W), which are regulated under International Convention for the Prevention of Pollution from Ships Annex IV. Both BAL-W and BIL-W samples were analysed in the study. Many of the microplastic (MP) particles detected in the BAL-W samples were micro sized, while the majority of MPs found in the BIL-W samples were macro (>0.5 mm) and micro (1 µm-<5 mm) in size. The findings show that MPs constitute the majority (53%) of the plastics analysed, followed by 25% mesoplastics and 11% nanoplastics (NPs). Plastics with a size class of 50-300 µm were most abundant in both BAL-W and BIL-W. For BAL-W and BIL-W sources, the average MP sizes were calculated to be 0.025-4.99±0.050 mm and 0.05-0.1±0.050 mm, respectively. Rubber/commercial (PNEU), polyethylene (PET) terephthalate, polystyrene (PS), and polyoxymethylene (POM) were the most abundant polymer types found in the BIL-W samples, accounting for 47.82%, 10.86%, 9.78%, and 6.55%, respectively, while PNEU and PE were the most abundant polymer types found in the BAL-W samples, accounting for 22.91% and 7.98%, respectively. The pollution load index was calculated 7.75 (Hazard Category IV) and 12.17 (Hazard Category V) for BAL-W and BIL-W waters. It is now clear that the BAL-W management system needs to be evaluated to eliminate MP pollution due to the presence of polymers in BIL-W and BAL-W.

Keywords: Marine environmental protection, MARPOL 73/78 Annex IV, sewage from ships, microplastic pollution, pollution load index (PLI)

1. Introduction

The massive amounts of plastic in the world's seas and oceans create a serious hazards to their natural ecological live. It is anticipated that 0.8 to 23.0 million tons of plastic wastes are floating in the seas and oceans [1]. Micro and macroplastics (MPs) contribute significantly to marine plastic pollution. With the increase in global maritime trade, the number of merchant ships is growing every year. As more ships transport, in addition to environmental degradation on land, pollution from ships is growing. The pieces of plastic are categorized based on their size: mesoplastics (5-25 mm), MPs (1-5 mm; MPs), and nanoplastics (<1 µm; NPs) [2-4]. MPs, particularly NPs, are tiny particles that may cause a variety of impacts on marine and coastal organisms. Ingestion of these plastics may threaten marine organisms' growth, survival, and reproduction [5]. They may also be hazardous to human health since they accumulate in seafood [6].

Address for Correspondence: Asst. Prof. Emrah Şık, İstanbul Technical University Faculty of Maritime, Department of Basic Sciences, İstanbul, Türkiye
E-mail: emrahs@itu.edu.tr
ORCID ID: orcid.org/0009-0000-1202-0314

Sources of pollution reaching the seas and oceans include terrestrial origin (44%), atmospheric pollution (33%), pollution from maritime activities (12%), waste and sewage dumping (10%), and offshore drilling and mining (1%) [7,8]. While terrestrial or anthropogenic pollutants are the main sources, pollutants from ships also contribute signific antly to marine pollution. The International Convention for the Prevention of Pollution from Ships (MARPOL 1973/78) is the core international maritime convention adopted by the International Maritime Organization (IMO) to prevent both operational and accidental pollution [9]. The Convention consists of six technical Annexes covering various aspects of marine pollution prevention, e.g., oil, toxic liquids, garbage, and emissions. Two of these annexes are "Annex I. Regulations for the Prevention of Pollution by Oil" and "Annex IV: Prevention of Pollution from Ship Sewage." In addition, The ballast water (BAL-W) Management Convention or BWM Convention (2004) is a treaty adopted by the IMO in order to help prevent the spread of potentially harmful aquatic organisms and pathogens in ships' BAL-W. According to all, the discharge of ship sewage also contributes to marine pollution. Sewage, greywater, debris, oil/water separator effluent, cooling water, boiler and steam generator blow-down, and bilge water (BIL-W) are examples of waste streams on ships [10]. Among these, BAL-W is important for its water-capacity, BIL-W is another waste source with high pollutant potential due to ship operational processes (the engine room and leaks or maintenance operations etc.). Therefore, these two wastewater types were chosen for this study.

Marine pollution is widely described as the hazardous migration of substances or energy that alters physical, chemical, or biological characteristics due to human activity (MARPOL Convention, 1973/78) [11]. However, in this context, organisms carried in BAL-W are regarded as biological agents rather than "substances". BAL-W and BIL-W are regarded as critical vectors for the spread of various pollutants, including MPs, across the world's seas [12,13]. MPs are synthetic plastic particles less than 5 mm in diameter that are persistent and non-biodegradable in the environment [14,15]. These particles not only represent physical pollution, but also threaten the health of ecosystems as they act as carriers for toxic chemicals, heavy metals, and pathogenic microorganisms. BAL-W and BIL-W, in particular, are thought to be key sources of conveyance for the spread of biological pollution and pollutants in the marine environment. However, barely anything has been revealed about the plastics included in BAL-W and BIL-W.

BAL-W: Maritime traffic continues to increase, with around 51,400 merchant ships in operation worldwide and around 3 to 5 billion tons of BAL-W carried by ships every year [7]. Today, BAL-W is one of the most important maritime pollutants and is associated with about one third of documented infestations worldwide. One of the biggest challenges for maritime transport is to find safe solutions for BAL-W management that minimize the environmental impact. To address this issue, following its regular meetings, the IMO has revised Annex IV of MARPOL 73/78 and made it mandatory for large ships to be equipped with a BAL-W management system (BWMS) from September 2025 [11]. This reduces the potential of invasive species spreading as a result of ships discharging untreated BAL-W. However, these waste waters, which are discharged and distributed in vast amounts across the world, are only disinfected for microbiological causes (Table 1) [16,17]. It still allows for the transfer of other pollutant factors, such as MPs. During ballasting, large amounts of seawater are pumped into the ballast tanks of ships. As a result, various creatures and particles prevalent in the maritime environment, including plastics, enter the ballast tanks with the brine and accumulate. Consequently, the collection of BAL-W from polluted territories could lead in MPs entering the port of destination when water treatment does not occur out [18]. In this way, MPs might contribute to marine pollution by BAL-W or BIL-W during marine transportation and act as a reservoir of pollutants.

To meet discharge standards, almost all ships are expected to be equipped with BWMS. Although various technologies such as filtration, chlorination, ozonation, pasteurization,

Table 1. IMO D-2 ballast water discharge standard.

Parameter	The limits for the indicators in the ballast discharge	
	USCG standards [10]	IMO D2 standards [4]
Zooplankton, organisms ≥50 µm	<1 viable organisms/100 m^3	<10 viable organisms/m^3
Phytoplankton, organisms 10-50 µm	<1 viable organisms/100 mL	<10 viable organisms/mL
Vibrio cholerae	<1 CFU/100 mL	<1 CFU/100 mL
Escherichia coli	<126 CFU/10 mL	<250 CFU/100 mL
Enterococci	<33 CFU/100 mL	<100 CFU/100 mL

CFU: Colony-forming unit, IMO: International Maritime Organization, USCG: United States Coast Guard and ultraviolet radiation (alone or in combination) are used for water purification [19,20], these are not effective methods for combating MP pollution. Studies have found that the average content of MPs in ship BAL-W and seawater samples were 12.53 and 11.80 units/L, respectively, with a high concentration of MPs in the 50-300 µm size class. The findings identified the main sources of MPs (such as BAL-W), their transport pathways and the associated ecological risks to marine ecosystems [12].

BIL-W: Various harmful substances, consisting of MPs and heavy metals, might enter the sea from ships through a variety of sources, including grey water, wastewater, ship cooling water, and treated sewage. Wastewater from regular ship operations persists and poses a significant risk to coastal aquatic ecosystems [21,22]. The wastewater has a pH range of 6.8 to 9.0, a salinity of 25 to 35 g/L, an oil concentration of 36 to 2953 mg/L, and a high chemical oxygen demand> 3-15 g/L [23]. In addition, studies have found MPs in wastewater [12]. For these reasons, strict environmental regulations on wastewater discharges and the tendency to reuse treated water make wastewater treatment a critical factor. MARPOL 73/78 regulates BIL-W management, limiting oil content to ≤15 mg/L when discharged into the sea. The literature reports on various types of BIL-W treatment methods, including coagulation, flocculation, membrane filtration, electrocoagulation, flotation, and combinations of these processes [24,25].

In addition, investigations have demonstrated that MPs accumulate in a variety of marine animals [26-28], and because of their small size, these particles can be ingested by a wide range of marine organisms [12]. Also, MPs have the ability to adhere to a variety of marine contaminants, including heavy metals, and accelerate their build up in the marine environment [29,30]. Human exposure to MPs and other contaminants that build up in marine food webs may have negative consequences [14]. All of this emphasizes how our seas are affected by MP contamination. Although there is few research on the migration of MPs through BAL-W, there aren't many on the migration of MPs through BIL-W. BAL-W and BIL-W pollutants, which have been studied in small quantities for MPs [12].

The aims of this study were to investigate MPs abundance and their characteristics, including size, polymer type, and chemical composition, in the BAL-W and BIL-W of ships, and to determine the pollution load index (PLI) of MPs in the BAL-W and BIL-W.

2. Materials and Methods

2.1. The Sampling Stations

The sampling work was conducted from April to September, 2024. There were seven sampling stations (Table 1) set up, 4 BAL-W and 3 BIL-W in the different type of ships, and seven waste water samples from ship-originated were obtained by collecting sample at each station. The vessels from which water samples were selected at random from three seas: the Black Sea, the Mediterranean Sea, and the Marmara Sea, regardless of type or tonnage. Table 2 shows information about each of the ships that were sampled for ship sewage, and Table 3 shows the physical and chemical measurement results of the samples. The BAL-W volume of the ships ranged from 500 m^3 to 10,000 m^3.

2.2. Sample Collection

Samples were collected from 7 sampling station (Table 3) as vertically water column. BAL-W sampling depth varied from 2 m to 6 m, while the BIL-W samples were taken from a depth of around 1 m below the surface. For this purpuse, 7 samples the volumes are given in Table 2, were collected with containers to include MPs. Then all the samples were transferred into the glass bottle and treated with hydrogen peroxide (30% v/v, Merck, Germany) to in order to remove organic material [31-33]. The bottles were rinsed several times with ethanol before use. Checked for any potential contamination occurring in the sample in the field and laboratory. Water samples were stored in dark and cold conditions until MP analysis.

Table 2. Information on the sampled ships.

Station	Matrix	Date	Type of vessel	GRT	BWMS	Sampling location	Sample volume (L)
1	BAL	31.09.2024	Oil tanker	3225	D2 UV/filter	Mediterranean/Italy/Ravina	5
2	BIL	31.09.2024	Oil tanker	3225	-	Mediterranean/Italy/Ravina	5
3	BAL	18.05.2024	Chemical tanker	3776	D2 UV/filter	Novorossysk/Russia	5
4	BAL	18.05.2024	Chemical tanker	3776	D2 UV/filter	Novorossysk/Russia	5
5	BIL	04.04.2024	Cargo	1554	-	Tuzla/İstanbul/Türkiye	3
6	BIL	25.04.2024	Tugboat	939	-	Tuzla/İstanbul/Türkiye	3
7	BAL	01.09.2024	Cargo	1243	-	Mersin/Türkiye	5

2-BAL: Dry cargo ship pre-BWMS sample, 3-BAL: Dry cargo ship post-BWMS sample, BIL: Bilge, BAL: Ballast

Table 3. Physical and chemical analysis results of ship sewage samples.

Station	Matrix	pH (-)	Conductivity (mS)	Salinity (g/kg)	Method
1	BAL	7.80	41.3	30.8	Vertical water column
2	BIL	8.20	1.33	0.78	
3	BAL	8.26	34.0	26.7	
4	BAL	8.22	34.6	26.6	
5	BIL	8.24	7.25	0.28	
6	BIL	7.80	2.64	0.25	
7	BAL	8.65	54.9	41.6	

2.3. Analysis

The polymer type of each presumed MP particle was determined by attenuated total reflection Fourier-transform infrared spectroscopy (micro-ATR-FTIR) at the laboratory. The samples were passed through a cellulose pre-filter and then filtered through 13 mm diameter aluminium oxide membrane filters with a 0.1 µm pore size (Whatman Cytiva Anodisc, Germany) into glass petri dishes. The collected samples were left under a fume hood for 2 hours and prepared for measurement with the micro-FTIR device. This technique produces high-quality spectral images of sample areas, with a pixel resolution of 6, 25, 25, or 50 micro meters. The dried filters were stored in a dust-free environment until the time of analysis. The filters were scanned in the imaging mode of the Perkin Elmer FTIR Spotlight 400 device using the Spectrum Image application (optical imaging), and transmittance measurements (chemical imaging) were taken across the entire filter surface. The chemical imaging was performed within a 10 mm x 10 mm area, scanning a 200 µm x 200 µm surface in the IR spectrum range of 690-4000 cm^{-1} using the Spectrum 3 application. Spectra were compiled after applying atmospheric correction, and data processing (MP mapping) was carried out using the siMPle application (Aalborg University-Denmark, Alfred-Wegener Institute-Germany). The results compiled from the siMPle application were used to create a MP distribution table.

2.4. PLI

This method has been commonly employed in earlier investigations of heavy metal pollution in sediment [34,35], and researchers are currently applying it for assessing the risk of MPs [36-38]. The PLI is a standard method for observing and evaluating pollution levels at various locations.

Tomlinson et al. [39] (1980) developed the pollutant load index. The PLI calculates pollution load by taking into account various contaminants (e.g., all metals) at various location. It is a basic geometric mean for the pollution factor (*CF*). The *CF* is calculated according to Equation 1 [40].

$$CF = CF_i / C_o \tag{1}$$

In Equation 1, *CF*; CF_i and C_o are the observed concentration of MPs at sampling location and the lowest concentration/background value of MP detected in the sample, respectively.

The PLI was derived with Equation (2):

$$\mathrm{PLI} = \prod_i^n \left(CF_i \right)^{0.5} \tag{2}$$

Where *i* represents a sample, *n* represents the number of samples, C_i represents the abundance of plastic in sample *i*, and C_o represents the lowest element concentration found in the accessible literature [41]. However, in the lack of background data from similar environments, the lowest baseline limit for MP abundance identified in this study was set at 0.05 units/m^3 based on data from the study conducted by Mutuku et al. [42] (2024) in five major oceans.

3. Results and Discussion

3.1. MPs Size Distribution from Ship-Sewage

MPs were detected in all BAL-W and BIL-W samples. The BAL-W and BIL-W samples presented in Figure 1 and Figure 2 included 96 and 92 plastic particles, respectively. Figure 2 shows the mean number of MPs in BAL-W and seawater. MPs amounts in the BAL-W and BIL-W samples were 5.28 (±3.57) and 6.20 (±3.20) items/L, respectively. There was no significant difference (p-value> 0.05) in the number of MPs between BAL-W and BIL-W. The abundance of MPs in the bilge tanks of the ships was moderately higher (36±4.99 items/L) than in the ballast tanks (5.0±1.39 items/L) (Figures 1 and 2).

The Persian Gulf (Bushehr port and Assaluyeh port) found concentrations ranging from 5.53 to 21.6 items/m^3 [12], whereas our concentrations in the BAL-W samples were similarly level with a range between 4.8 to 27 items/m^3. Furthermore, research by Matiddi et al. [43] investigated levels of MP in the BAL-W of nine commercial ships and found values ranging from 100 to 1410 items/m^3, with a mean of 651 items/m^3.

The BAL-W samples contained 55.6.0% particles between 25 and 50 µm, 38.8% with particles larger than 50 µm, and 5.6% with particles smaller than 25 µm. But, 48.0% of the

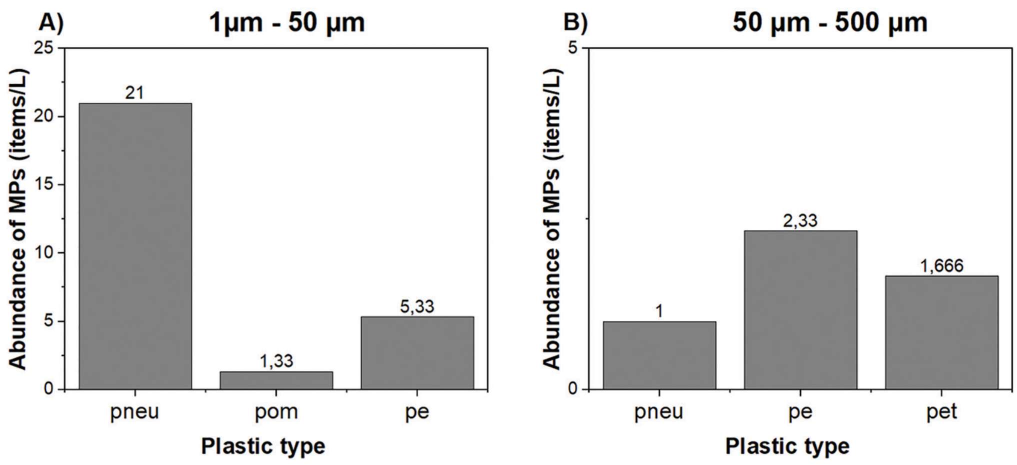

Figure 1. Types of plastic in BAL-W according to size classes 1-50 μm, and 50 -500 μm.

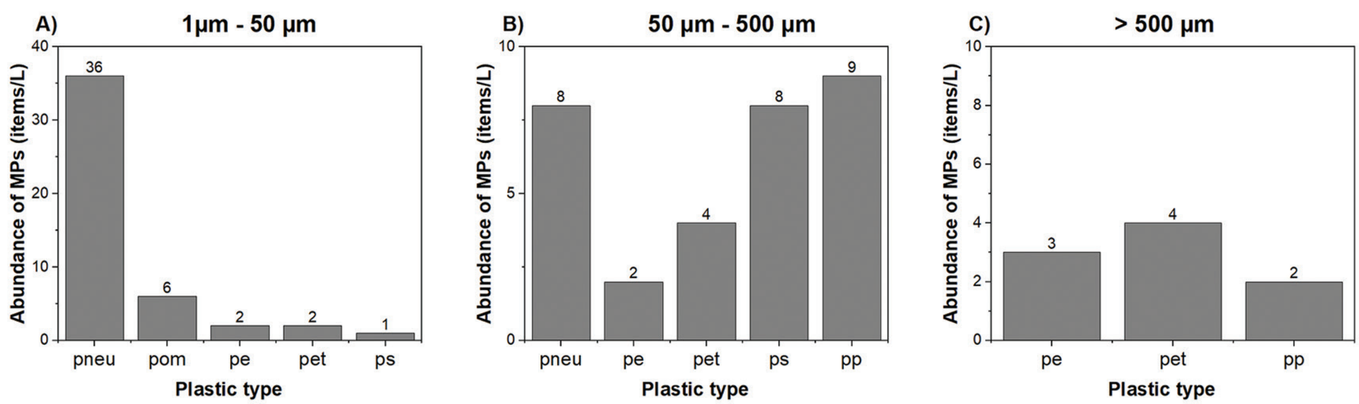

Figure 2. Types of plastic in BIL-W according to size classes 1-50 μm, 50 -500 μm, and >500 μm.

plastics in the SS samples were 0.05-0.1 mm particles, 24.0% were 0.1-0.25 mm particles, and the remaining 28% were plastics larger than 0.25 mm. Previous research found that MPs were most prevalent in seawater in the Persian Gulf, Iran [44], Caspian Sea, Iran [45], and Marmara Sea, Türkiye [46] with sizes of 1000-3000, 1000-5000, and 1-100 μm, respectively.

In BAL-W operations, the point of intake is critical. The plastic particle count per unit volume in the ballast sample is predicted to be high when the ballast intake occurs in a hub or busier port. Conversely, the plastic count density will be low in port locations with limited capacity. Terrestrial pollution is also influenced by the port area's population density and residential layout.

Remarkably high abundances of mezo and macro particles were found in two bilge samples (5 and 6), up to 4.69 and 15.33 items/L. However, 1.55 to 4.8 μm/L particles were quantified in the ballast tank, which is also located in the 7th sample. In samples 5 and 7, which show the highest plastic abundance, it is noticeable that these two sampling sites are commercial port areas with heavy shipping traffic. It is assumed that the intensive commercial activities, population density, and terrestrial contaminants in these areas have contributed to the increase in plastic density.

Particularly in aquatic bodies, MPs gradually degrade into smaller MP and even NP fragments due to regular abrasion [47]. An enormous major threat in the proliferation of these small plastic particles is their potential hazard to organisms that continuously ingest them and their bioaccumulation in living organisms [48,49]. Based on this objective, it is anticipated that the elements of ship sewage tanks might add to the MP pollution that is already there and spread the related chemical and biological pollutants. It is crucial to note that MPs are effective vectors for the transport of heavy metals and chemical pollutants across many miles. The presence of MPs in the marine environment, may migrate to enter of MPs and connected contaminants into food chains and eventually ingested by human [50]. Therefore, it is stressed to adopt strict regulations to minimize MP levels in ship sewage tanks before discharge through effective treatment systems [51].

3.2. Chemical Characterization of Microplastics

This study investigated the presence of MPs in the BAL-W and BIL-W of ships sailing in various seas and ports. The 188 plastic particles in the BS and SS samples belong to six polymer types: polyethylene (PE), polyethylene terephthalate (PET), polyoxymethylene (POM), polypropylene (PP), polystyrene (PS), and Rubber/commercial (PNEU). The chemical composition of the plastics has been confirmed using micro-FTIR spectroscopy. Figure 3 displays the color codes for the different polymer types observed in the BAL-W and BIL-W samples. However, particles containing protein, cellulose, crustaceans and etc. have been excluded from the particle count. Our study of the MP samples from the ship sewage indicates that the main constituent is PNEU (rubber/commercial), with POM and PET being the other two typically identified polymers. PNEU and POM are engineering thermoplastics used for manufacturing specific components with high stiffness, low friction, and superior dimensional stability. Seals and rubbers are commonly utilized in marine machinery and auxiliary operations for both static and dynamic applications. PNEU pneumatic systems provide several advantages. Furthermore, POM polymer is employed in high-performance technical components such as tiny gears, ball bearings, skid plates, fasteners, clamps, and locking mechanisms. As therefore, long-lasting polymers like POM and PNEU are chosen in corrosive and abrasive conditions like seawater. In contrast, PET is generally used in areas such as the food industry, beverage packaging, packaging film, plastic boxes, kitchenware, mechanical engineering and packaging. It is also a preferred material in the manufacture of moving parts that operate under high pressure. Unlike PNEU and POM, emissions in ship-sourced wastewater are assumed to be caused by human or essential activity. Although the maritime environment contains a wide range of plastics, MPs such as polyvinyl chloride, PP, PE, PS, PET, and polyamide are prevalent [32,54]. According to published studies, the most popular polymer types in the Persian Gulf of Iran are PE, PET, and nylon [53], PP and PE are the most prevalent polymer types in the surface waters of China's Yellow Sea region [53], and nylon is the most prevalent polymer type in Antarctica's Ross Sea [46]. For example, pneumatic rubber fenders are used in ports and on ships to minimize structural damage in the event of collisions [54]. However, the rubber broken from these collisions can enter the marine ecosystem and be carried into the tanks during ballast transportation. The findings of this study are coherent with previous studies, but also provide new details about BIL-W that have been little discussion thus far. The differences in the abundance of MPs and the types of polymers may be due to various factors such as traffic, fishing and marine tourism on various coasts of the world.

While most MP particles were observed in BAL-W samples 7 and 1 in Figure 4a, the particles in BIL-W samples 1 and 4 were mostly micro- and mesoplastic (Figure 4b). While sample 2 contained more plastic fragments (Figure 5b), sample 5 contained predominantly mesoplastic particles (Figure 5a). The BIL-W samples contained fewer particles in the 1-5 mm size range, while the BAL-W samples had the most particles in the <50 mm range.

The findings of this investigation indicated that MPs were not eliminated by the BAL-W disinfection system, and that both wastewaters included polymers of various types and sizes.

3.3. Risk Assessment of MP PLI

Pollution indexes are widely used to assess plastic pollution in aquatic and terrestrial environments [38,55]. These indexes provide a quantitative framework for assessing pollution levels and potential ecological risks [37]. As macro-, micro- and NPs mostly originate from anthropogenic sources, the determination of a reference background level (C_o) for the assessment of plastic pollution remains a crucial challenge [56]. As there are no defined standards for assessing for

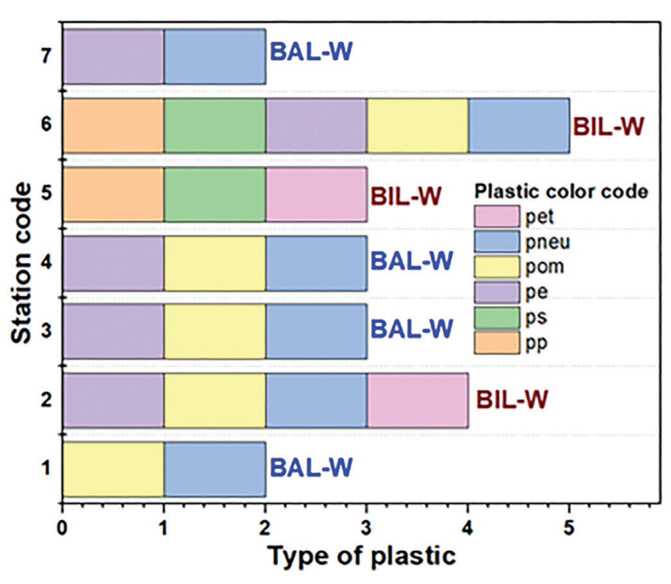

Figure 3. Distribution of MPs detected in ship-sewage sample.

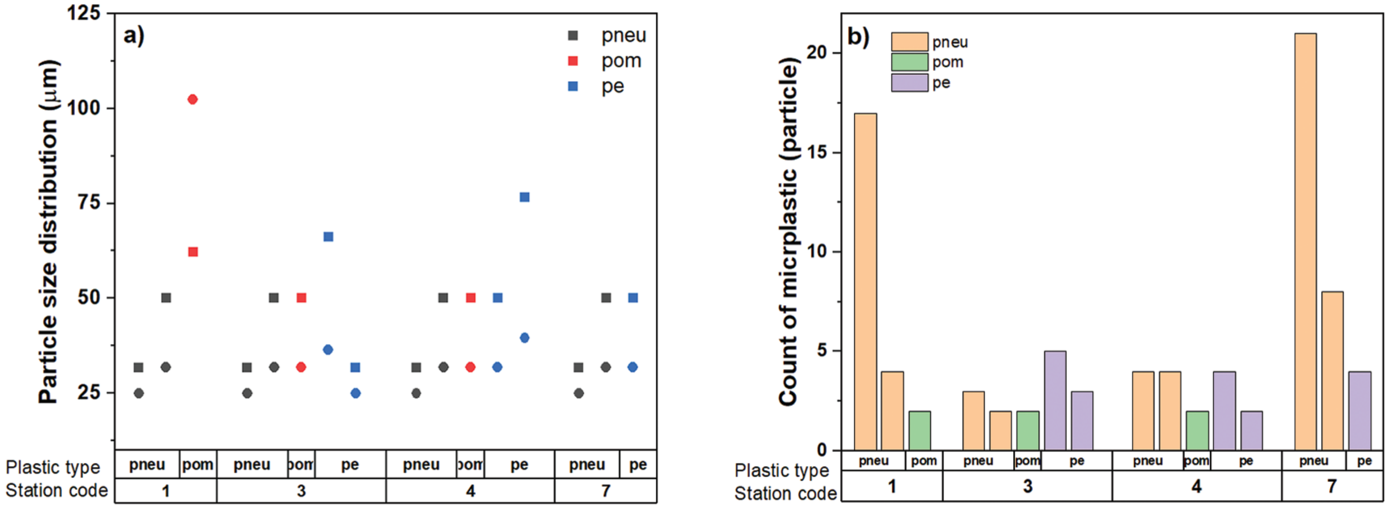

Figure 4. MP analysis in ballast water samples a) size distribution by species, b) Count of MPs.

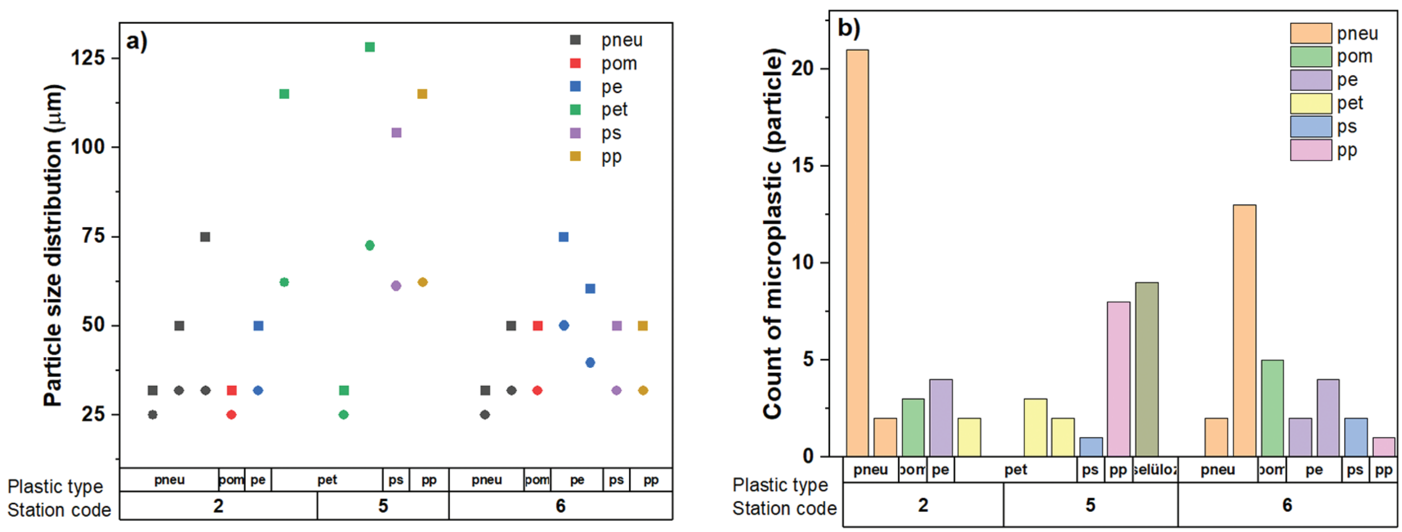

Figure 5. MP analysis in bilge water samples a) size distribution by species, b) Count of MPs.

the risk assessment of plastics, the results of the PLI largely depend on the chosen reference background value of plastic abundance [57]. However, these reference values may vary considerably from study to study. Some research employs probabilistic analytical values based on species sensitivity distributions [58], whereas others utilize the minimal abundance values at the sampling site as baseline concentrations [59]. These methodological inadequacies contribute to large variations in PLI-based risk evaluations for MPs [55]. The concentration of MPs in the seas varies from 0.002 to 22 pc/m^3, revealing a skewed distribution. The average concentration was highest in the Atlantic Ocean (2.58 pc/m^3) and lowest in the Southern Ocean (0.04 pc/m^3) [42].

Table 4 represents the PLI calculated for the BAL-W and BIL-W samples. The estimated pollutant load index indicated significant pollution risks in two BAL-W samples and a very high pollution risk in five samples. A high PLI score indicate the region is contaminated with MPs.

The calculated PLI values for all BIL-W samples were $10.2 \leq$ PLI <12.17, indicating a very high level of very high pollution (Hazard Category V). The calculated PLI values for BAL-W ranged from Hazard Category IV to Hazard Category V. This type of risk assessment for ship sewage

Table 4. Pollution load index (PLI) calculated for BAL-W and BIL-W samples.

Station	Matrix	CF	PLI	Hazard Level
1	BAL	92	9.6	V, very high pollution
2	BIL	148	12.17	V, very high pollution
3	BAL	60	7.75	IV, significant pollution
4	BAL	64	8.0	IV, significant pollution
5	BIL	104	10.2	V, very high pollution
6	BIL	128	11,3	V, very high pollution
7	BAL	132	11.5	V, very high pollution

C_o: The lowest value found in the literature was set at 0.05 units/m^3. BIL-W: Bilge water, BAL-W: Ballast water, *CF*: Pollution factor.

is unique to this study; similar results have been reported for Categories IV and V in urban sewage [60] and seawater [61,62]. Previous research by Dar and Gani [55] (2025) has found that the PLI ranged from 3.9 (Hazard Category I) to 40 (Hazard Category IV), indicating that glaciers are moderately to severely polluted. The findings of the PLI of MPs reveal that the environmental impact of MP pollution in the oceans, as well as the contribution of ship sewage (BAL-W and BIL-W), represent a significant risk to marine ecosystems. BAL-W and BIL-W wastewater may transport MP particles and pollutants in these plastics between ports.

In addition, MP fragments have the potential to be significant carriers of pollutants [63,64]. These transports can retain pollutants on their surfaces through physical adsorption, depending on potential pollutants such as heavy metals, pharmaceuticals, etc., in the regional marine and ocean ecosystem, and even transfer them to marine organisms or humans that feed on them.

Based on the findings of this study, BIL is an important source of MPs, as it is exposed to intense pollution from ship auxiliary operational processes. BAL is also a potential source of MPs, which can act as a carrier of these particles and related pollutants between different ports and could potentially have harmful effects on the marine environment, aquatic organisms, and, consequently, human health. As a result, macro-, micro-, and NPs are capable of acting as vectors for pollutant transmission, hence their inclusion as an environmental impact element in ship sewage regulations (e.g., MARPOL Annex I or Annex IV) is beneficial and raising awareness is necessary in the maritime sector.

4. Conclusion

The micro-FTIR analysis of BAL-W and BIL-W samples conducted in this work revealed that ship sewage poses a serious environmental risk in terms of MP pollutants. The most prevalent polymers identified in BAL-Ws were POM, PNEU, and PET, whereas POM, PET, PS, and PNEU were found in BIL-Ws. The abundance of MPs in the bilge tanks of the ships was moderately higher (37±0.7 particles/L) than in the ballast tanks (24.0±1.0 particles/L). We concluded that the MP content in BIL-W is often higher than in BAL-W, making BIL-Ws popular places to find MP pollution due to the impacts of various operational and natural factors, such as tank position, personnel activities, environmental conditions, waves, and wind, causing bilge tanks more prone to the accumulation of large amounts of MP. The findings reveal that the BWMS implemented by the IMO as part of the MARPOL Convention for the Protection of the Marine Environment are insufficient for eliminating MPs contamination.

According to the pollutant load index, ship-sewage from BAL-W and BIL-W is rated as Hazard Category IV (significant pollution) and Hazard Category V (extreme pollution), causing serious environmental risk. All of the study's findings highlight the importance of ships in sea ecosystem, as well as their far-reaching influence as a result of their many interactions with the environment. The findings of this study, which focus on the kind and concentration of MPs that collect in ship sewage, can be utilized as primary data to inform future research on the impact of MPs on ships. Based on the findings of the study, it is recommended to implement effective waste management systems, introduce stricter regulations, and raise marine sector awareness.

Footnotes

Financial Disclosure: The author declared that this study received no financial support.

References

[1] M. Strokal, P. Vriend, M. P. P. Bak, C. Kroeze, J. van Wijnen, and T. van Emmerik, "River export of macro- and microplastics to seas by sources worldwide", *Nature Communications,* vol. 10, no. 14, pp. 4842, Aug 2023.

[2] P. Madala, A. Waikar, and H. Parate, "Detection to remediation: strategies for managing microplastic pollution in freshwater systems", *International Journal of Computational and Experimental Science and Engineering*, vol. 11, no. 3, pp. 5301-5316, 2025.

[3] GESAMP, "Sources, fate and effects of microplastics in the marine environment: a global assessment", (Kershaw, P.J., ed.). Rep. Stud. GESAMP, 90-96, 2015.

[4] A.L. Andrady "The plastic in microplastics: a review", *Marine Pollution Bulletin,* vol. 119, no. 1, pp. 12-22, Jun 2017.

[5] M. Cole, C. Lindeque Halsband, and T. S. Galloway, "Microplastics as contaminants in the marine environment: A review", *Marine Pollution Bulletin*, vol. 62, no. 12, 2588-2597, Dec 2011.

[6] M. R. M. Zaki, and A. Z. Aris, "An overview of the effects of nanoplastics on marine organisms", *Science Total Environmental*, vol. 20, no. 831, pp. 154757, 2022.

[7] M. Čović, B. Bacalja, M. Krčum, and G. J. Mrčelić, "From ballast water to harmful air emissions: how to reduce the impact of shipping on the pollution of the marine environment -a review", *WIT Transactions on The Built Environment,* vol. 204, pp. 105-116, Sep 2021.

[8] G. Potters, Marine Pollution. Bookboon, 1st edition. ISBN 978-87-403-0540-1, 2013.

[9] IMO (International Maritime Organization), "International convention for the control and management of ships' ballast water and sediments", London, BWM/CONF/36, London, U.K. 2004.

[10] WHO, Guide to ship sanitation. 3rd edition. World Health Organization; 2011.

[11] M. Convention, "International convention for the prevention of pollution from ships", *MARPOL Conventional Outlet.* 1973. http://www.imo.org

[12] A. Zendehboudi, et al. "Analysis of microplastics in ships ballast water and its ecological risk assessment studies from the Persian Gulf", *Marine Pollution Bulletin*, vol. 198, pp. 115825, Jan 2024.

[13] M. Arienzo, L. Ferrara and Marco Trifuoggi, "The dual role of microplastics in marine environment: sink and vectors of pollutants", *Journal of Marine Science Engineering*, vol 9, pp. 642, Jun 2021.

[14] A. Anthony, "Microplastics in the marine environment", *Marine Pollution Bulletin*, vol. 62, no. 8, pp. 1596-1605, Aug 2011.

[15] L. Peng, D. Fu, H. Qi, C.Q. Lan, H. Yu, & C.bGe, "Micro-and nano-plastics in marine environment: source, distribution and threats — a review", *Science of the Total Environment,* vol. 698, 134254, Jan 2020.

[16] U.S. Environmental Protection Agency (EPA), "*Generic protocol for the verification of ballast water treatment technology*", version 5.1. In: Report Number EPA/600/R-10/146. United States Environmental Protection Agency, Washington, DC. 2010.

[17] Global TestNet, "Ballast Water Management system", 2021. https://globaltestnet.org/our-work.html

[18] U.S. Coast Guard, "In: standards for living organisms in ships' ballast water discharged in U.S. waters", Final Rule. FR, 77, 17254-17304, 2012.

[19] E. Tsolaki, and E. Diamadopoulos, "Technologies for ballast water treatment: a review", *Journal of Chemical Technology & Biotechnology,* vol. 85, no. 1, pp. 19-32, Jan 2010.

[20] W. A. Gerhard, K. Lundgreen, G. Drillet, R. Baumler, H. Holbech, and C.K. Gunsch, "Installation and use of ballast water treatment systems – implications for compliance and enforcement", *Ocean & Coastal Management*, vol. 181, no. 1, 104907, Nov 2019.

[21] J. Lloret, N. Zaragoza, D. Caballero, and V. Riera, "Impacts of recreational boating on the marine environment of Cap de Creus (Mediterranean Sea)", *Ocean & Coastal Management,* vol. 51, no. 11, pp. 749-754, 2008.

[22] O. V. Malakhov, O. M. Palagin, A. I. Naydyonov, K. A. Lytkhoglyad, and A. V. Bondarenko, "Bilge and oily water treatment during operation of vessel", *TransNav,* vol. 18, no. 2, pp. 433-445, 2024.

[23] J. Church, et al. "Identification and characterization of bilgewater emulsions", *Science of the Total Environment*, vol. 691, pp. 981-995, Nov 2019.

[24] M. Han, J. Zhang, W. Chu, J. Chen, and G. Zhou, "Research progress and prospects of marine oily wastewater treatment: a review", *Water,* vol. 11, no. 12, pp. 2517, Nov 2019.

[25] S. Soeprijanto, D. F. Nury, and L. Pudjiastuti, "Treatment of oily wastewaters from Tanjung Perak Port by electrocoagulation using aluminium electrodes", *IOP Conference Series: Materials Science and Engineering*, vol. 543, 012098, Jun 2019.

[26] X. Li, et al. "From marine to freshwater environment: a review of the ecotoxicological effects of microplastics Ecotoxicology*", Journal of Environment and Safety*, vol. 251, pp. 114564, Feb 2023.

[27] M. Cole, P. Lindeque, E. Fileman, C. Halsband, and T. S. Galloway, "The impact of polystyrene microplastics on feeding, function and fecundity in the marine copepod Calanus helgolandicus", *Environmental Science and Technology,* vol. 49, no. 2, pp. 1130-1137, Jan 2015.

[28] D. Neves, P. Sobral, J.L. Ferreira, T. Pereira, "Ingestion of microplastics by commercial fish off the Portuguese coast", *Marine Pollution Bulletin,* vol. 101, no. 1, pp. 119-126, Dec 2015.

[29] F. Haque, and C. Fan, "*Microplastics in the marine environment: a review of their sources, formation, fate, and ecotoxicological impact*", Chapters, in: Monique Mancuso & Teresa Bottari & Ahmed A. Abdelhafez & Mohamed Abbas (ed.), Marine Pollution - Recent Developments, IntechOpen. pp. 1-33, 2022.

[30] J. Kang, L. Zhou, X. Duan, H. Sun, Z,Ao, S. Wang, "Degradation of cosmetic microplastics via functionalized carbon nanosprings", *Matter,* vol. 1, no. 3, pp. 745-758, Sep 2019.

[31] C. B. Crawford, and B. Quinn, "*Microplastic collection techniques",* In: Crawford CB, Quinn B (eds) Microplastic pollutants. Elsevier, pp. 179-202, 2019.

[32] V. Hidalgo-Ruz, L.G. Richard, C. Thompson, M. Thiel, "Microplastics in the marine environment: a review of the methods used for identification and quantification", *Environmental Science & Technology,* vol. 46, pp. 3060-3075, Mar 2012.

[33] T. Rocha-Santos, M.F. Costa, "Catherine Mouneyrac, Handbook of Microplastics in the Environment", pp. 6-16, *Springer Nature Switzerland AG*, ISBN 978-3-030-39041-9 (eBook), 2022.

[34] H. Effendi, M. Kawaroe, D.F. Lestari, "Ecological risk assessment of heavy metal pollution in surface sediment of Mahakam Delta East Kalimantan", *Procedia Environmental Science*, vol. 33, pp. 574-582, 2016.

[35] K. Rezaee Ebrahim Saraee, M. R. Abdi, K. Naghavi, E. Saion, M. A. Shafaei, and N. Soltani, "Distribution of heavy metals in surface sediments from the South China Sea Ecosystem, Malaysia", *Environmental Monitoring Assessment*, vol. 183, no. 1-4, pp. 545-554, Dec 2011.

[36] X. Li, et al. "From marine to freshwater environment: a review of the ecotoxicological effects of microplastics, *Ecotoxicology Environmental Saf*ety, vol. 251, 114564, Feb 2023.

[37] Z. Pan, Q. Liu, R. Jiang, W. Li, X. Sun, and H. Lin, "Microplastic pollution and ecological risk assessment in an estuarine environment: the Dongshan Bay of China", *Chemosphere,* vol. 262, pp. 127876, Jan 2021.

[38] P. Xu, G. Peng, L. Su, Y. Gao, L. Gao, and D. Li, "Microplastic risk assessment in surface waters: a case study in the Changjiang Estuary, China", *Marine Pollution Bulletin,* vol. 133, pp. 647-654, Aug 2018.

[39] D.L. Tomlinson, J.G. Wilson, C.R. Harris, and D.W. Jeffrey, "Problems in the assessment of heavy-metal levels in estuaries and the formation of a pollution index", *Helgoländer Meeresuntersuchungen*, vol. 33, no. 1, pp. 566-575, Mar 1980.

[40] L. Hakanson, "An ecological risk index for aquatic pollution control.a sedimentological approach", *Water Research,* vol. 14, no.8, pp. 975-1001, 1980.

[41] A. H. M. E. Kabir, M. Sekine, T. Imai, K. Yamamoto, A. Kanno, and T. Higuchi, "Assessing small-scale freshwater microplastics pollution, land-use, source-to-sink conduits, and pollution risks: perspectives from Japanese rivers polluted with microplastics", *Science of the Total Environment,* vol. 768, pp. 144655, May 2021.

[42] J. Mutuku, M. Yanotti, M. Tocock, and D. H. MacDonald, "The abundance of microplastics in the world's oceans: a systematic review", *Oceans,* vol. 5, pp. 398-428, Jun 2024.

[43] M. T. A. Matiddi, C. Silvestri, A. M. Cicero, and E. Magaletti, "First evidence of microplastics in the ballast water of commercial ships", *Fate and Impact of Microplastics in Marine Ecosystems From the Coastline to the Open Sea,* pp. 136-137, Jan 2017.

[44] K. Kor, and A. Mehdinia, "Neustonic microplastic pollution in the Persian Gulf", *Marine Pollution Bulletin,* vol. 150, pp. 110665, Jan 2020.

[45] A. Manbohi, A. Mehdinia, R. Rahnama, and R. Dehbandi, "Microplastic pollution in inshore and offshore surface waters of the southern Caspian Sea", *Chemosphere,* vol. 281, 130896, Oct 2021.

[46] V.Z. Sönmez, C. Akarsu, and N. Sivri, "Impact of coastal wastewater treatment plants on microplastic pollution in surface seawater and ecological risk assessment", *Environmental Pollution,* vol. 318, 120922, Feb 2023.

[47] M. Cole, H. Webb, P. K. Lindeque, E. S. Fileman, C. Halsband, and T. S. Galloway, "Isolation of microplastics in biota-rich seawater samples and marine organisms", *Scientific Reports,* vol. 4, no. 4528, pp. 1-8, Mar 2014.

[48] L. G. A. Barboza, A. D. Vethaak, B. R. Lavorante, A. K. Lundebye, and L. Guilhermino, "Marine microplastic debris: an emerging issue for food security, food safety and human health", *Marine Pollution Bulletin,* vol. 133, pp. 336-348, Aug 2018.

[49] N. Von Moos, P. Burkhardt-Holm, A. Köhler, "Uptake and effects of microplastics on cells and tissue of the blue mussel Mytilus edulis L. after an experimental exposure", *Environmental Science and Technology,* vol. 46, pp. 11327-11335, Oct 2012.

[50] R. K. Naik, P. Chakraborty, P. M. D'Costa, N. Anilkumar, R. Mishra, and V. Fernandes, "A simple technique to mitigate microplastic pollution and its mobility (via ballast water) in the global ocean", *Environmental Pollution,* vol. 283, pp. 117070, Aug 2021.

[51] S. Dobaradaran, F. Soleimani, I. Nabipour, R. Saeedi, and M. J. Mohammadi, "Heavy metal levels of ballast waters in commercial ships entering Bushehr port along the Persian Gulf", *Marine Pollution Bulletin,* vol. 126, pp. 74-76, Jan 2018.

[52] A. Naji, M.A. Nuri, "Microplastics contamination in molluscs from the northern part of the Persian Gulf", *Environmental Pollution,* vol. 235, pp. 113-120, Apr 2018.

[53] X. Sun, J. Liang, M. Zhu, Y. Zhao, and B. Zhang, "Microplastics in seawater and zooplankton from the Yellow Sea", *Environmental Pollution,* vol. 242, pp. 585-595, Nov 2018.

[54] S. M. Park, H. Jin Kim, H. Rim Cho, K. Hwan Kong, D. Kyeom Park, and J. K .Paik, "Effect of pneumatic rubber fenders on the prevention of structural damage during collisions between a ship-shaped offshore installation and a shuttle tanker working side-by-side", *Ships and Offshore Structures*, vol 18, no. 4, pp. 596-608, 2023.

[55] S. A. Dar, and K. M. Gani, "Deciphering the source contribution of microplastics in the glaciers of the North-Western Himalayas", *Journal of Hazardous Materials*, vol. 491, 137975, Jul 2025.

[56] M. Ranjani, et al. "Assessment of potential ecological risk of microplastics in the coastal sediments of India: a meta-analysis", *Marine Pollution Bulletin*, vol. 163, 111969, Feb 2021.

[57] Z. Yin, "The pollution of microplastics in sediments: the ecological risk assessment and pollution source analysis", *Science of the Total Environment*, vol. 859, 160323, Feb 2023.

[58] H. Yang, F. Sun, H. Liao, Y. Guo, T. Pan, and F. Wu, "The pollution of microplastics in sediments of the Yangtze River Basin: occurrence, distribution characteristics, and basin-scale multilevel ecological risk assessment", *Water Research,* vol. 243, 120322, Sep 2023.

[59] K. K. Riya, et al. "Characteristics, contamination levels, and ecosystem risk assessment of microplastics in surface water of a highly urbanized river from a developing country", *ACS Omega*, vol. 9, no. 52, pp. 50922-50932, Dec 2024.

[60] S. Hajiouni, et al. "Occurrence of microplastics and phthalate esters in urban runoff: a focus on the Persian Gulf coastline", *Science of Total Environmental,* vol. 806, no. 1, 150559, Feb 2022.

[61] P. Prarat, and P. Hongsawat, "Microplastic pollution in surface seawater and beach sand from the shore of Rayong province, Thailand: distribution, characterization, and ecological risk assessment", *Marine Pollution Bulletin,* vol. 174, 113200, Jan 2022.

[62] D. Lithner, A. Larsson, and G. Dave, "Environmental and health hazard ranking and assessment of plastic polymers based on chemical composition", *Science of the Total Environment,* vol. 409, pp. 3309-3324, Aug 2011.

[63] G. Liu, Z. Zhu, Y. Yang, Y. Sun, F. Yu, and J. Ma, "Sorption behavior and mechanism of hydrophilic organic chemicals to virgin and aged microplastics in freshwater and seawater", *Environmental Pollution,* vol. 246, pp. 26-33, Mar 2019.

[64] M. J. Stapleton, A. J. Ansari, and F. I. Hai, "Antibiotic sorption onto microplastics in water: a critical review of the factors, mechanisms and implications", *Water Research,* vol. 15, no. 233, 119790, Apr 2023.

RESEARCH ARTICLE
DOI: 10.54926/jnamt.2025.2528
J Nav Architect Mar Technol 2026;228:11-23

Analysis of Operational Drivers of Unscheduled Downtime in a Container Fleet

Araks Ekmekçioğlu

Yıldız Technical University Faculty of Naval Architecture and Maritime, Department of Marine Engineering, İstanbul, Türkiye

To cite this article: A. Ekmekçioğlu. Analysis of operational drivers of unscheduled downtime in a container fleet. *J Nav Architect Mar Technol*. 2026;228:11-23.

Received: 19.09.2025 - **Revision Requested:** 10.10.2025 - **Last Revision Received:** 17.12.2025 - **Accepted:** 24.12.2025 - **Publication Date:** 19.01.2026

Abstract

Unplanned downtime in liner shipping undermines voyage reliability and increases costs. This study systematically compiles 397 unplanned downtime events in a container ship fleet between 2017 and 2021, standardizing them according to system/subsystem and time/location attributes. A risk score consisting of frequency × duration × impact components was defined to quantify the severity of downtime on the operation. Pareto analysis was applied to identify a small number of critical causes. Variables driving downtime were extracted using a Classification and Regression Tree (CART) model and supported by Ward's linked hierarchical clustering. The findings show that 89% (352/397) of downtimes were propulsion/propulsion system-related, representing approximately 1,460 hours of the total 1,767 hours; main engine events predominated in this group with 256 incidents and ~730 hours. Despite their rarity, shaft/propeller/stern-tube failures lead to very long delays per event (≈96 hours on average). CART outputs reveal that the longest downtimes are associated with fuel pump and injection failures (median ≈153.6 hours), while exhaust and lubrication-related failures are also high-impact. Pareto analysis showed that oil mist detector (OMD) related events accounted for 63.1% of the total risk, fuel injection 14.8%, and exhaust 7.9%; these three factors accounted for 85.8% of the risk. The findings suggest prioritizing fleet wide condition-based maintenance packages, targeted spare parts management, exhaust gas trend monitoring, rigorous OMD calibration/validation flows, and role-based training programs across the fuel, exhaust, and lubrication triad. Key indicators should be defined to track annual downtime reductions of ≥10-15% in critical clusters and improvements in diagnostic speed.

Keywords: Unscheduled downtime, Marine propulsion failures, CART decision tree, Pareto analysis

1. Introduction

Maritime transport, which constitutes a large part of global trade, is a strategic sector in a race against time. Ships engaged in container transport in the maritime industry are operated with the goals of on-time delivery, high operational efficiency, and low downtime. However, due to the nature of maritime operations, unplanned downtime is sometimes unavoidable. These stoppages can occur for a wide variety of reasons, such as technical failures, environmental conditions, operational errors, or maintenance negligence, and consequently lead to significant time losses and damage costs.

While there is a significant body of literature on ship malfunctions across diverse areas, such as predictive maintenance, statistical analysis of accident data, and human and organizational factors, these studies often focus on single systems or the single-ship scale, and limited fleet-scale downtime assessment based on event records remains limited. While recent studies have demonstrated the technical potential of data-driven/hybrid approaches for main engine

Address for Correspondence: Asst. Prof. Dr. Araks Ekmekçioğlu, Yıldız Technical University Faculty of Naval Architecture and Maritime, Department of Marine Engineering, İstanbul, Türkiye
E-mail: araks@yildiz.edu.tr
ORCID ID: orcid.org/0000-0002-4821-0272

and auxiliary systems (e.g., risk prioritization, maintenance scheduling, contextual effects), the integration of these methods with real-world field incidents in container ship fleets and the direct translation of findings into maintenance prioritization and role-based training planning have not yet been sufficiently demonstrated. In the Turkish context, empirical evidence that quantitatively maps downtime causes at the fleet scale and translates the results into fleet management decisions is lacking. This study aims to fill this gap with a workable framework that organizes field-sourced incident data at the fleet level, introduces risk concentration (Pareto) and waiting time determinants [Classification and Regression Tree (CART)], and links the resulting patterns to condition-based maintenance and role-based training priorities.

The existing literature covers a wide range of topics, focusing on technical system failures and maintenance strategies that cause unplanned downtime. In academic studies on similar topics, predictive maintenance models for ship systems play a critical role in anticipating potential field failures and ensuring uninterrupted ship operations. Kalafatelis et al. [1] noted that artificial intelligence (AI)-supported predictive maintenance systems in the maritime sector have great potential, particularly in terms of preventing failures in main engines and auxiliary equipment. Budimir et al. [2] developed models for optimizing maintenance scheduling using Weibull and Markov-based analyses. A comparative study by Tinga et al. [3] demonstrates how data-driven and physics-based prognostic models can be used in fleet management. Shen et al. [4] aimed to automatically extract information from written text in maintenance/failure records for the rapid identification of malfunction causes and symptoms on ships. They used the graph transformer networks to capture important fragments of the text (e.g., “failure cause”, “symptom”, “equipment name”).

Operationally, Karmelić et al. [5] examine disruptions that reduce voyage reliability in container liner shipping, using both literature and internal operational reports, classifying delay causes into four tiers: land transport, anchorage, port, and cruise. Nguyen [6] has demonstrated with mathematical models that optimal maintenance planning under limited resources and time can directly reduce unplanned downtime. In studies focusing on the human factor, Islam et al. [7] emphasized the triggering effect of environmental influences and organizational deficiencies on human error in maintenance processes. Specifically for Türkiye, Ünlügençoğlu [8] analyzed maritime accidents and statistically evaluated the relationship between human error and equipment failure.

Unplanned stoppages can occur not only during navigation but also during port operations and under the influence of environmental factors. Romano-Moreno et al. [9] linked stoppages at ports to meteorological data, demonstrating that operational planning must include these factors. Millefiori et al. [10] analyzed the effects of coronavirus disease-2019 on global maritime transport, illustrating the pressure of extraordinary conditions on operational continuity.

The system-level literature offers greater technical depth. Simion et al. [11] argued that AI-based predictive maintenance solutions for ship machinery provide efficiency in terms of reliability. Soltani Motlagh et al. [12] and Jimenez et al. [13] reported that the integration of physics-based models with machine learning in propulsion systems provides high accuracy in fault detection. BahooToroody et al. [14] used Gaussian Process Latent Variable Model and Bayesian inference to non-parametrically model the prediction of ship machinery failure risk. The model provides strong evidence for Pareto-based diagnosis and adaptive maintenance planning under uncertainty. Onwuegbuchunam et al. [15] developed models related to the temporal distribution of shaft and gearbox failures. Crankcase explosion risk and oil mist detectors (OMD). Numerical/computational studies of crankcase explosions and experimental research examining the morphological characteristics of oil mist particles provide direct evidence for determining OMD thresholds and reducing false alarms [16,17]. These findings provide a framework for why unplanned downtime originating from the main engine are critical in terms of both safety and operational time. At the critical subsystem level, thermal behavior and wear in stern tube bearings, risk prioritization in boiler systems [18,19], and duty cycle effects in deck equipment [20] have been identified as factors directly contributing to unplanned downtime.

In studies related to hull damage and structural reliability, reliability studies on critical load conditions such as strength comparisons between damaged/intact states and asymmetric bending in container ships confirm from a structural perspective that a limited number of events can produce very high downtime durations [21]. Network and dynamic impact analyses link to maintenance and operational planning by showing how reliability limits change in operational scenarios [22]. Modeling accident data using Bayesian approaches also enables learning cause-effect relationships and prioritizing “high impact–low frequency” risks [23,24].

Taken together, these strands offer robust methods and mechanisms, yet there is limited empirical, fleet-scale synthesis of forced stoppages grounded in incident records—particularly for Turkish container-ship fleets. Our study addresses this gap by organizing field data at fleet level, quantifying risk concentration (Pareto) and waiting-time drivers (CART), and mapping the results to actionable levers for maintenance planning and role-specific training.

This study aims to reveal which systems and subsystems experience the highest concentration of unscheduled downtime events based on five years of records from 50 container ships, and which factors explain the duration of these stops. The research question can be summarized as follows: "Which technical clusters drive the most unplanned stoppages at the fleet level, and which variables are more influential in determining the level of downtime?" To this end, recorded technical stoppages were examined. The 397 incidents identified over the five-year period were coded in a standardized manner according to systems and subsystems. Subsequently, a Pareto analysis was performed using risk scores derived from the frequency-duration-impact components of the events to identify the critical minority, and CART regression was used to extract the variables and threshold distinctions explaining the waiting time. The findings were interpreted through the decision tree structure and importance scores. The objective is to reveal frequently recurring failure patterns, evaluate the impact of these outages on operational performance, and develop recommendations that will contribute to maintenance, training, and fleet management processes based on the results.

This study examines in detail the forced downtime events that occurred on the ships of a shipping company with a container ship fleet between 2017 and 2021. Unplanned downtime during navigation and port operations over a five-year period involving a fleet of 50 ships was analyzed in terms of both technical causes and operational and training impacts. The aim is to identify recurring failure patterns, assess the impact of these stoppages on operational performance, and develop recommendations to contribute to maintenance, training, and fleet management processes based on the findings.

2. Materials and Methods

2.1. Study Area and Data Set

Unplanned downtime events of a private maritime company with a large container ship fleet based in Türkiye were examined over a 5-year period. The company operates 50 vessels and manages Türkiye's largest fleet in this field. The vessels are actively engaged in various trade routes worldwide.

The dataset was created by compiling and digitizing unplanned downtime reports prepared by ship personnel by the company's technical department. The dataset records variables such as ship name, date, duration and location of the stoppage, system/component name, and reason for the stoppage for each event. A total of 397 unplanned downtime events were recorded.

The data was compiled from technical maintenance and incident report forms obtained from the company's operational reporting system. The incidents were digitally entered into the system by engineers on board and ship technical superintendents, who are marine engineers and fleet managers. Standardized analysis tables were created from this raw data. Each incident was classified according to technical category. Within the three main operational categories (propulsion system, cargo operations, and mooring operations), the propulsion system-related issues with the highest number of incidents were divided into subcategories and analyzed in detail.

This study uses incident records from a single Turkish container-ship fleet operating predominantly on liner trades. While this yields high internal consistency (common procedures, documentation standards, and engine families), it constrains external validity in several ways. First, risk concentrations and waiting-time drivers may differ in fleets with distinct operating profiles, vessel types (tanker, bulk carrier, ro-ro), class/age distributions, or propulsion configurations. Second, the dataset intentionally excludes non-technical delays (e.g., weather, port/terminal operations); this design choice isolates technical stoppages but can inflate their relative share of total downtime and limits comparisons with studies using all-cause delays. Third, organization-specific maintenance practices (spares policies, OMD calibration routines, training cadence) may alter shipboard crew competency skills.

Only recorded technical downtimes were included in the analysis. Unreported minor interruptions were excluded from the study; unexpected technical failures that caused operational disruptions were considered. Planned maintenance, adverse weather conditions, port operational delays, or externally caused downtimes were excluded from the analysis; the focus was on technical downtimes. Data processing included data cleaning and categorization. Incomplete, inaccurate, or duplicate records were eliminated.

2.2. Analysis Method

The analytical framework adopted in this study is designed to balance methodological rigor with operational interpretability. Rather than maximizing predictive accuracy through black-box models, the focus is placed on transparent, rule-based methods that allow failure mechanisms and downtime drivers to be directly interpreted by fleet managers and marine engineers. Pareto analysis is employed to identify risk concentration and critical subsystems at the fleet level, while the CART algorithm is used to uncover threshold-based relationships and nonlinear patterns governing downtime duration. This combined approach enables both prioritization of dominant failure modes and actionable insights for maintenance planning and role-based training, grounded in real operational data.

2.2.1. Risk assessment and pareto analysis

Risk scores were calculated for each type of failure to determine the impact of failures on the operational efficiency of ships. Risk scores were determined using a weighted scoring method based on the frequency of occurrence, duration of the failure, and its operational impact. The Pareto chart created using these scores visually demonstrated the dominant effect of main engine failures on waiting time. Pareto analysis was applied to confirm the finding that approximately 80% of the total downtime is concentrated in approximately 20% of the failures.

2.2.2. CART algorithm

The CART algorithm was used to analyze the effects of ship main engine failures on ship waiting times. CART is a powerful and flexible machine learning approach widely used in classification and regression problems [25]. In the regression context, CART creates a binary decision tree structure that iteratively partitions the dataset into two subsets to identify the relationship between variables.

The modeling process begins by treating the entire dataset as a single node (root node). The algorithm then partitions the dataset into two subsets by determining the most appropriate independent variable and threshold value that minimizes the variance or mean square error (MSE) of the target variable. This process continues iteratively until one of the predefined stopping criteria is met (e.g., maximum tree depth, minimum terminal node size). In the final stage, the mean value of the target variable at each terminal node (leaf node) is assigned as the predicted value for all observations belonging to that node.

The CART model, being a nonparametric method, is highly effective in capturing nonlinear relationships between variables. Furthermore, the model's visualizability and interpretability facilitates easy understanding for both technical and operational stakeholders in decision-making processes. In this study, model performance was evaluated using R^2 (coefficient of determination), root MSE (RMSE), MSE, mean absolute deviation (MAD), and mean absolute percentage error (MAPE) statistics.

In addition, a dendrogram analysis was performed using Ward's linkage method and the Euclidean distance metric to support the findings obtained from the CART model. This approach measures the similarity between failure types to form hierarchical clusters, thereby enabling a visual classification of the relationships among different categories of engine failures.

3. Findings

3.1. General Situation: Summary of the Number of Downtime

During the five-year evaluation period, a total of 397 unscheduled downtime events were recorded in the container ship fleet under review. These stoppages were grouped under three main operational categories: Propulsion System, Cargo Operation, and Mooring Operation activities.

When examining the distribution of stoppages by system, as shown in Figure 1, 89% of downtimes (352 incidents) were due to propulsion systems. Stoppages during cargo operations accounted for 10% of unplanned stoppages, with 39 incidents. The remaining 1% (6 incidents) occurred during mooring operations.

Table 1 shows the total number of stoppages and durations by category. The total unplanned stoppage duration was calculated to be approximately 1,767 hours over the five-year period. The duration distribution is also parallel to the number of incidents.

Based on these data, the average duration of a downtime is calculated to be approximately 4.5 hours. Across the fleet, the annual average number of unplanned downtimes per vessel is approximately 1.6. When the average main engine

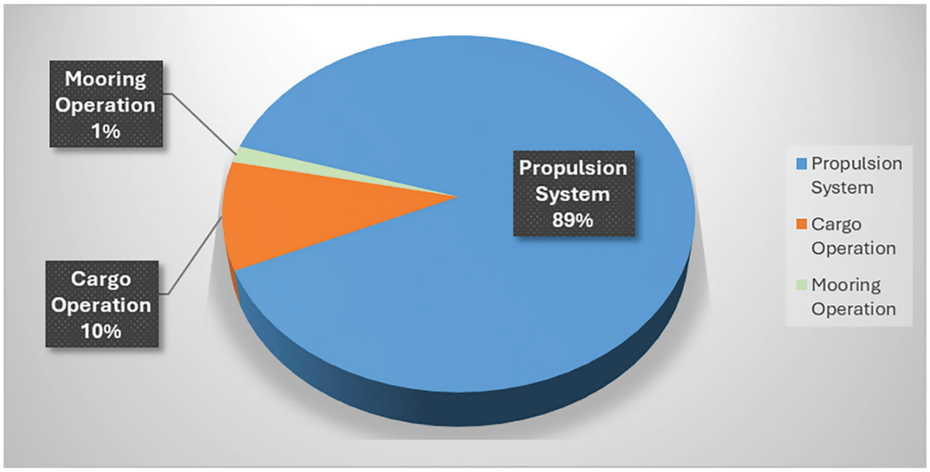

Figure 1. Distribution of stoppages by system.

operating time is assumed to be 4,200 hours per year, the ratio of time spent on downtime to total sailing time is approximately 0.15%. While this low ratio indicates that fleet operations are generally planned and controlled, it also points to the need for priority intervention in terms of propulsion system failure density, maintenance planning, and technical training.

3.2. Distribution by Cause of Downtime

Of the 397 unplanned downtimes that occurred during the five-year period under review, 89% (352 incidents) were directly attributable to propulsion systems. This high percentage highlights how critical main propulsion systems are to operational continuity on container ships.

Based on this criticality, stoppages related to propulsion systems were detailed in terms of their technical components. The propulsion system data, shown in Table 2 with a total of 352 incidents and 1,460 hours of downtime, was broken down into subsystems and analyzed.

Due to the combined reporting of some incidents, mandatory downtime caused by main propulsion systems has been divided into nine main technical categories. This analysis aims to contribute to fleet management, maintenance planning, and technical training content by identifying the subsystems where downtime is concentrated.

In this distribution, main engine failures are clearly ahead not only in terms of the number of incidents but also in total downtime duration. The entire propulsion system alone accounted for approximately 50% of the downtime, with a total of 730 hours of downtime across 256 incidents. The most frequently recurring issues include fuel injection problems, fuel pump (FP) failures, and problems caused by the exhaust system.

In contrast, although only 4 incidents occurred in the propeller, drive shaft, stern tube, and bow thruster group, the total downtime was quite high at 384 hours. This group, with an average downtime of 96 hours per incident, shows that these system failures are rare but cause very long operational interruptions. In such cases, the complete operational downtime of the ship brings with it commercial losses as well as safety risks. These types of failures usually require the ship to wait in port for weeks for repairs. Emergency intervention is not possible; dry docking is usually required. Therefore, these components are considered critical priority. Preventive vibration analysis, oil analysis programs, and proactive maintenance scheduling are vital for this type of system failure.

Some systems with relatively few incidents stand out due to their singular impact. Specifically, in the “Hull/Fire/Maneuvering” category, despite only 8 incidents, the total downtime was 116 hours, with an average interruption of 14.5 hours per incident. This finding demonstrates that some infrequent failures have a high operational impact.

Boiler systems stand out with a total of 151 hours of downtime across 33 incidents. The average downtime of 4.6 hours highlights the need for continuous maintenance and monitoring of this system. Especially, boiler tube perforations lead to prolonged port delays and deviations from estimated arrival times.

Twelve incidents occurred in the Piping, Valves, Pumps, Coolers, and Heaters group, resulting in a total of 36 hours

Table 1. Number of downtimes and durations by category.

	Propulsion system	Cargo operation	Mooring operation	Total
Total downtime (number)	352	39	6	397
Total downtime duration (hours)	1460	272	35	1767

Table 2. Summary of downtime in propulsion systems by subcategory.

Propulsion system	Number of incidents	Duration (hour)	Average duration
Automation & Alarm systems	7	4	0.6
Boiler system	33	151	4.6
Generator load sharing & Black out	25	19	0.8
Hull & Fire & Maneuvering	8	116	14.5
Main engine	256	730	2.9
Piping, valves, P/P, cooler/heater	12	36	3.0
Propeller & Shaft & Stern tube & Thruster	4	384	96.0
Others	7	20	2.9
Total	352	**1460**	**4.1**

of downtime. With an average downtime of 3 hours, these components are classified as medium priority. Diesel generator load sharing, automation and alarm systems, and other groups have a limited impact on propulsion system downtime, with both low frequency and low duration. Most failures in these systems were resolved in less than 1 hour per incident. Incidents under the "Other" category include delays due to GPS display errors, pitch control failures, rudder & pitch-controlled propeller system failures, and items recorded during flag state inspections in port.

As a result, not only the frequency of propulsion system stoppages but also their individual impacts and system-based temporal intensity should be considered in fleet management. In addition to the main engine, boiler systems, maneuvering control systems, and propeller structures are also highlighted as priority areas in terms of preventive maintenance, spare parts inventory management, and training.

3.3. Critical System Analysis: An in-Depth Look

Detailed analysis of fleet data shows that some technical systems fail more frequently than others and have a much greater operational impact. In this section, critical subsystems causing the most downtime or leading to long durations in individual incidents are analyzed separately. The aim is to provide targeted insights for optimizing fleet management and technical maintenance strategies. Table 3 presents the number of main engine failure incidents and their downtimes by subcategory.

In the critical system analysis, main engine-related failures were divided into subcategories and examined. CART regression analysis and hierarchical clustering (Ward-Linkage, Euclidean Distance) methods were evaluated together to determine the impact of main engine failures on ship downtime. The overall goal was to reveal the distribution of downtime events by main engine subcategories and to identify which systems most significantly impact operational continuity.

In the CART regression analysis, waiting time (in hours) was considered the dependent variable and failure types were considered the independent (explanatory) variables. The entire data set consisted of 11 different failure types, and the total number of events and average durations for each failure type were evaluated. The model was evaluated using the median and median absolute deviation (MAD) metrics, taking into account the distribution structure of the data and the sample size. This approach mitigated the impact of outliers in the data set, providing a more robust statistical representation.

Statistical performance metrics for the model generated using the CART method demonstrate that the analysis results have a strong predictive capacity. A total of four predictor variables were used in the resulting model, all of which were found to be statistically significant. The model's coefficient of determination (R^2=99.78%) indicates that almost all of the variance in the dependent variable can be explained. Furthermore, the error measures (RMSE=1.6601, MSE=2.7561, MAD=0.7304, MAPE=0.0377) were quite low. These results demonstrate that the model successfully predicts ship waiting times with high accuracy and low error (Table 4).

Figure 2 demonstrates the variation in model error, measured by Relative MAD, with respect to the number of terminal nodes. While increasing the number of nodes typically lowers the error rate, an excessive number of nodes can

Table 3. Number and duration of main engine incidents by subcategory.

Main engine failures	Number of incidents	Duration (hour)	Duration (day)
Oil mist detector	27	53.8	2.2
Fuel pump & Inj VV/Inj pipe	52	153.6	6.4
Fuel line & Fuel filter	24	60.3	2.5
Exhaust	44	96.1	4.0
Automation & Sensor failure	17	23.6	1.0
Lubrication system & Water in oil & LO filter	16	76.0	3.2
Cooling system & Cover	14	54.0	2.2
Piston & Rings	7	49.5	2.1
Start & Maneuvering & Governor system	24	76.1	3.2
Alpha lubricator	10	15.9	0.7
Other	21	71.3	2.9
Total	**256**	**730.2**	**30.4**

lead to model complexity and overfitting, thereby reducing the model's ability to generalize. Therefore, identifying the optimal trade-off is crucial. The analysis determined the optimal structure to be 8 terminal nodes, where the Relative MAD was minimized to 0.0291. At this optimal configuration, the correlation coefficient of the training set was calculated as 87.33%.

The regression tree generated as a result of the analysis is shown in Figure 3. At the root node of the tree (Node 1), the median waiting time for all faults was determined to be 60.25 hours. This value serves as a general indicator of performance across all fault types examined. The high median absolute deviation (MAD=25.13) indicates significant differences in waiting times across fault types.

The model categorizes failure types into two main groups. The main difference between these two groups is the median values in the waiting time distributions. The first group (Node 2) consists of failures with shorter waiting times on average, while the second group (Node 5) includes failure types characterized by longer waiting times. The first separation of the model was based on the "main engine event type" variable, which revealed two main groups. The first group represents events in the categories of alpha lubricator, automation & sensor, cooling system, fuel line & filter, OMD, piston & rings (Alp_Lub, Au_Sen, Cool, FL, OMD, Pist), while the second group includes events in the categories of exhaust, FP & injection valve (inj vv), lubrication system, other, and start & manuevring (Exh, FP, Lub, Other, Star). The median value for the first group on the left branch was calculated as 51.63, and for the second group on the right branch as 76.05. This shows that waiting times due to engine failures in the second group have a higher impact.

In particular, the median value for FP and valve failures was determined to be 153.64, standing out as the factor with the highest impact on the system. This clearly demonstrates that fuel injection system malfunctions are a key parameter significantly affecting downtime. Fuel injection line malfunctions (pump barrel and plunger wear, control rack/governor lockup, fuel valve nozzle clogging, common-rail pressure leaks, timing deviations) directly reduce cylinder combustion pressure and ignition quality. The resulting effects include power loss, unsteady combustion, exhaust temperature deviations, vibration, and the necessity of slowdowns/stoppages for safety reasons. Many interventions on the fuel injection system at sea can extend downtime due to the need for equipment cooling, fine-tolerance component replacement, calibration, testing procedures, or limited equipment and spare parts availability.

Similarly, faults related to the "Exhaust (Exh)" and "Lubrication (Lub)" systems were observed to have high median values. Because these are critical parameters that directly affect engine performance, they stand out as the most

Table 4. Performance metrics for the CART regression model.

Total predictors	4
Important predictors	4
Number of terminal nodes	8
Minimum terminal node size	1
R-squared	99.78%
Root mean squared error (RMSE)	1.6601
Mean squared error (MSE)	2.7561
Mean absolute deviation (MAD)	0.7304
Mean absolute percent error (MAPE)	0.0377

CART: Classification and Regression Tree

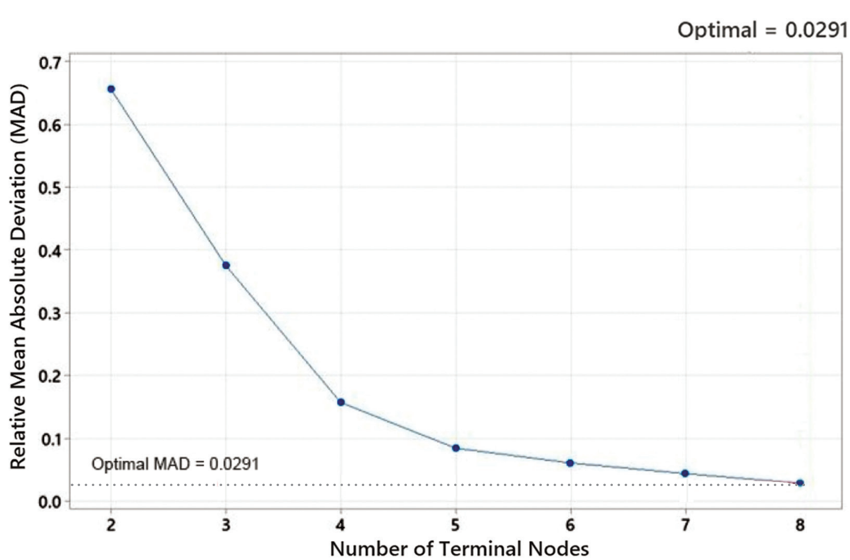

Figure 2. Optimization of the node.

significant contributors to downtime and require careful attention. It is technically expected that exhaust (Exh) and lubrication (Lub) faults produce high median downtime. Soot/oil carryover in the exhaust line, turbocharger fouling, or manifold and seal leaks increase back pressure, disrupting combustion. Safety measures such as power reduction/stop, cooling, cleaning, and rebalancing (turbo, sensor, insulation) prolong downtime. On the lubrication side, pressure drop/pump failure, filter blockage, viscosity and temperature deviations, or increased metal particles lead to critical scenarios such as bearing damage and the risk of crankcase explosion. This necessitates time-consuming interventions such as oil sample analysis, circuit checks, filter and cooler maintenance, and bearing inspections. In conclusion, Exh and Lub faults are critical parameters that directly affect engine performance.

In contrast, failures occurring in the “sub-components (Alp_Lub)”, “cooling (Cool)”, and “sensor (Au_Sen)” systems have lower median values. This result can lead to shorter downtimes due to the early detection of these failures and rapid intervention during maintenance processes. Failures in these three groups are generally localized and are quickly managed onboard using redundant/twin equipment (stand-by pumps, parallel heat exchangers), isolation valves, and modular component replacement. In cooling circuits, flow is maintained with a pump/heat exchanger switch-over; system safety is maintained by calibration/restart or rapid replacement on the sensor side; and in lubrication sub-components, filter replacement, leak repair, and bypass options shorten downtimes. Furthermore, since these failures are often detected with early warning (alarm), they can be deferred until port under power-limited operation rather than

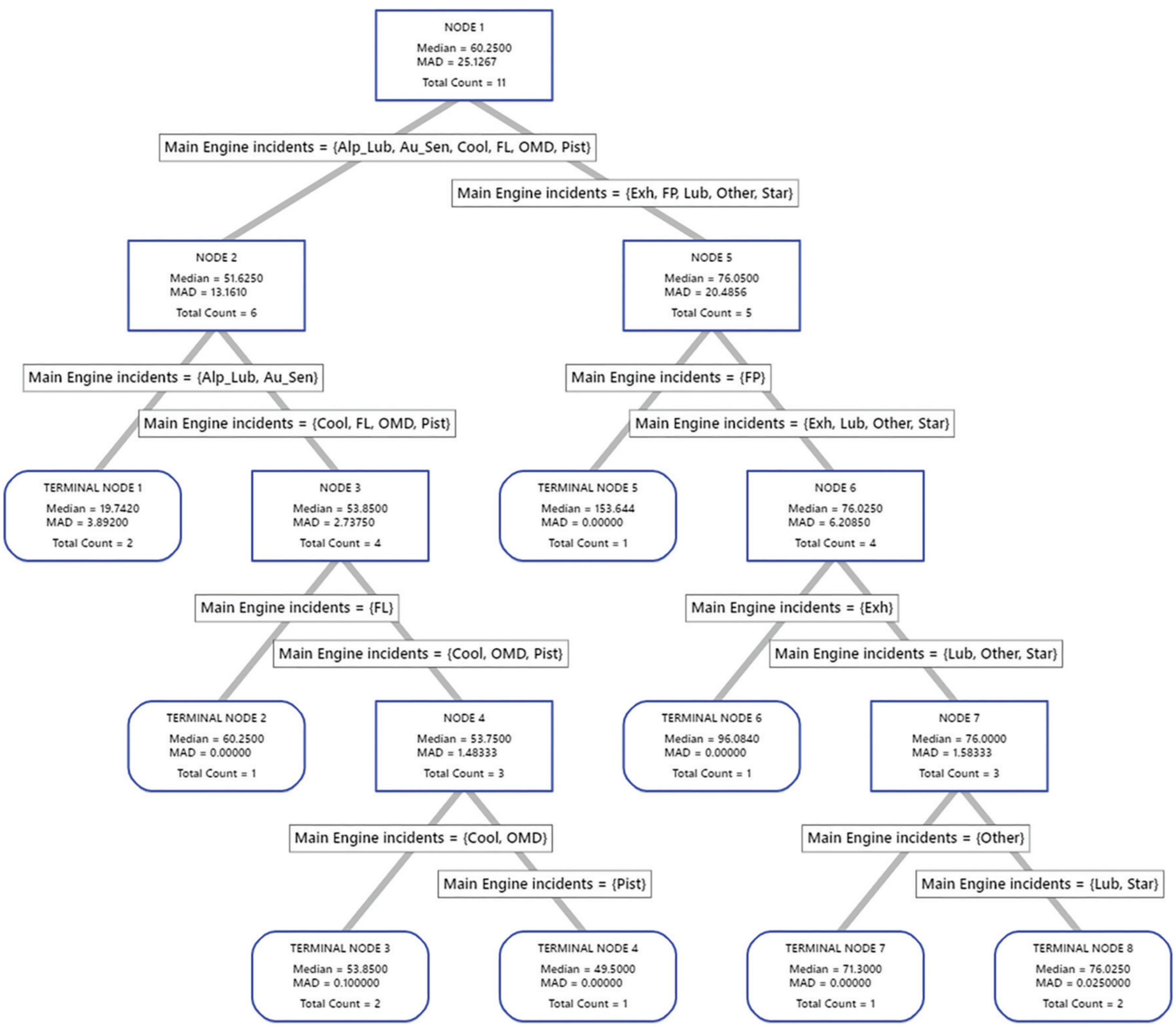

Figure 3. CART regression analysis results showing the effect of main engine failures on downtime.

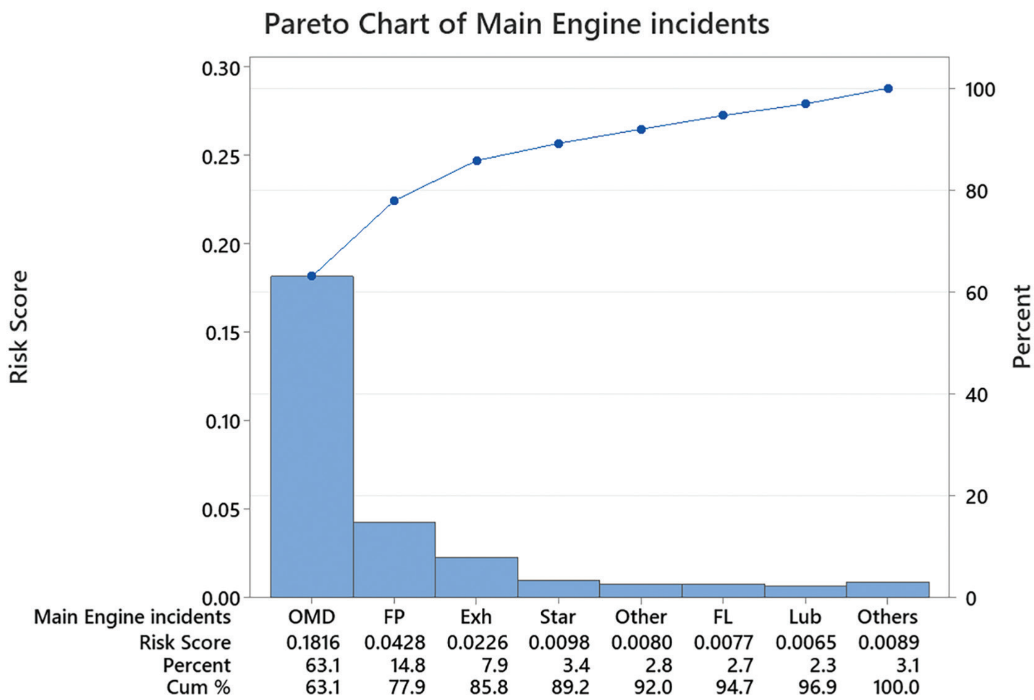

Figure 4. Pareto chart showing the severity of main engine failures according to risk scores.

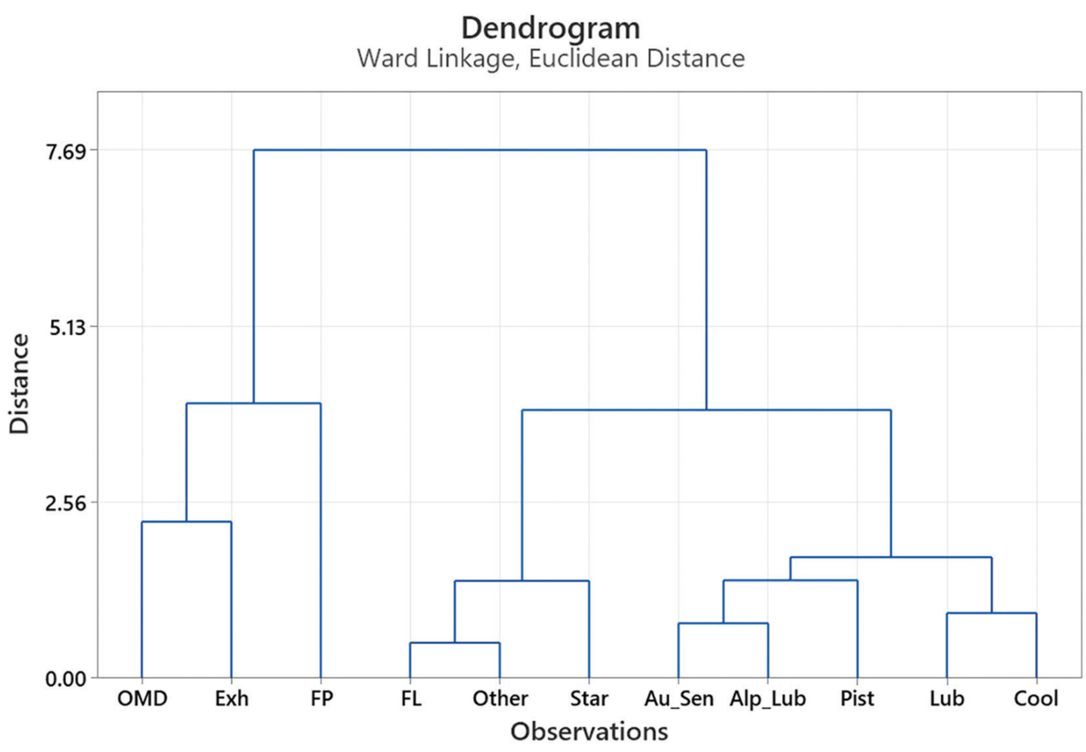

Figure 5. Dendrogram showing the similarity levels of fault types.

a full shutdown for safety reasons; consequently, downtimes are typically short.

Figure 4 shows a Pareto analysis of main engine failures. The graph shows the severity of failure types based on the risk score in ship operations. According to the analysis results, failures caused by OMD were identified as the most critical failure type, accounting for 63.1% of the total risk. This result demonstrates the crucial importance of regular maintenance and monitoring of OMD systems for main engine safety and operational continuity. OMD alarms are generally based on two factors: actual oil mist detection (crankcase fire risk, high density) or false alarms due to sensor sensitivity and air pressure adjustment. In these events, the operational impact is significant because the engine automatically shuts down or reduces speed. Often, the ship must be shut down until the alarm is verified. While some failures in these systems do not pose a real risk, each one triggers a maximum operational response due to safety protocols. Even if there is a sensor error, the engine must be shut down and the necessary checks performed seriously, just like the actual oil mist risk. A high-priority, critical alarm is due to the potential for major damage to the engine or a crankcase explosion. This demonstrates that factors such as calibration frequency of OMD systems, sensor quality, and crew diagnostic ability are critical for operational continuity.

OMD failures are followed by FP and valve failures (14.8%) and exhaust system (Exh) failures (7.9%). When these three failure types are considered together, they account for 85.8% of the total risk, indicating that operational disruptions in the majority of the system are caused by these components. Other failures (starting system, fuel leakage, lubrication system, etc.) constitute only less than 15% of the total risk.

This finding is consistent with the "80/20 Pareto principle" and demonstrates that preventive maintenance of critical components, particularly OMD, fuel, and exhaust systems, should be prioritized to improve system performance and reduce ship downtime.

Comparing the findings with those obtained through hierarchical cluster analysis (Figure 5), significant parallelism was observed between the two methods. The clustering of "OMD", "Exh", and "FP" failures within the same cluster in the dendrogram is consistent with the high median values of these parameters in the CART analysis. Similarly, the close clustering of "Cool", "Lub", and "Run" failures confirms the high correlation between these components due to common operating conditions (e.g., heat transfer and lubrication processes). Another cluster includes the auxiliary sensor (Au_Sen), alpha lubricator (Alp), and starting system (Star) failures, indicating that these failures are related to electronic control and monitoring systems.

4. Discussion

In this section, the findings obtained in the study are compared with similar studies in the literature and their operational implications are evaluated. The fact that 89% of the unplanned stoppages identified in the study were caused by propulsion systems reveals that ship operations are largely dependent on these systems. This finding coincides with the assessment in Vizentin et al.'s [26] study. Vizentin et al. [26] states that propulsion systems are the main source of failures in container ships, particularly concentrated in the main engine and shaft lines. The high failure rate poses a risk not only technically but also in terms of operational reliability. Numerical and experimental studies on the risk of crankcase explosions and the reliability of OMD provide concrete scientific evidence for optimizing detector threshold values and reducing false alarms by analyzing the morphological characteristics of oil mist particles in the crankcase [16,17].

Failures occurring in systems such as stern tube and propellers cause quite long downtimes despite being observed at low frequencies. This creates a special risk profile in terms of fleet management. A technical report prepared by Kuroiwa et al. [27] states that stern tube bearing failures are mostly caused by deterioration in lubrication systems, leaks in gaskets, and inadequate temperature control. Similarly, an experimental study by Chang et al. [28] showed that water-lubricated shaft sleeve bearings are sensitive to parameters such as temperature, load, and speed, and even a small tolerance deviation can cause long-term operational downtime. In this context, shaft sleeve and propeller systems should be considered strategic critical systems due to their high downtime, despite the low number of incidents.

The source of some unplanned stoppages of ships is not technical failure but rather faulty or overly sensitive alarm notifications from automation systems. In particular, "false positive" alarm events originating from OMD systems create uncertainty in the crew's decision-making mechanism and sometimes lead to unnecessary stoppages. Thorpe and Pabby's [29] comprehensive analysis indicates that the high sensitivity of OMD systems does not always provide a safety advantage; on the contrary, false alarms lead to a loss of confidence and psychological stress among the ship's crew. In this context, it is evident that topics such as alarm management and crew decision-making competence should be an integral part of technical training.

5. Evaluation and Results

This study systematically evaluated 397 unplanned downtimes recorded on container ships during the 2017-2021 period. The center of gravity of downtimes was the propulsion system (352 incidents; 89%), while cargo operations (39 incidents; 10%) and mooring downtimes (6 incidents; 1%) were among the remaining downtimes. Total unplanned downtime was calculated as 1,767 hours, with an average duration per incident across the fleet of approximately 4.5 hours. Downtimes related to the main engine alone, within the propulsion system, accounted for approximately half of the total duration, with 256 incidents and 730 hours.

A detailed examination of the main engine subtypes revealed that FP-injector, exhaust (Exh), and lubrication (Lub) failures were characterized by high median wait times, while cooling (Cool), sensor (Au_Sen), and subcomponent (Alp_Lub) failures were managed in relatively short times. In the CART regression tree, the root node began with a median wait time of 60.25 hours; after the decomposition, one branch corresponded to a median wait time of 51.63 hours, and the other to 76.05 hours. In this structure, the median for FP failures reached the highest value of ~153.64 hours, indicating that fuel injection failures significantly prolonged wait times. Hierarchical clustering results supported this picture; the close clustering of OMD-Exh-FP indicated a tendency toward long waits, while the association of Cool-Lub-Pist indicated a common behavior related to heat transfer and lubrication conditions. Pareto analysis showed that OMD-related events accounted for 63.1% of the total risk, FP for 14.8%, and Exh for 7.9%; these three items together reached 85.8%. This overall picture indicates that a small number of critical items at the fleet level drive a large portion of the total waiting time.

A condition-based maintenance package is recommended for the fuel-exhaust-lubrication triad, where risks are most pronounced. As a technical maintenance strategy, cyclical component replacement programs should be established fleet-wide for injectors, FPs, and exhaust components. To reduce both fuel and exhaust system problems, main engine performance values, especially maximum combustion pressure values, should be checked more frequently, and maintenance should be planned to anticipate potential problems.

On the fuel side, test bench calibration records for injection pumps/injectors should be regularly maintained. To save time in the event of malfunctions in these systems, especially based on competency, third- or fourth-level engineers should be trained and made aware of maintaining spare parts for replaceable fuel system components.

Exhaust gas temperature trend monitoring should be implemented in the exhaust; deviations above ±30 °C between cylinders can be detected before they reach alarm levels, enabling early intervention. To achieve this, implementing a checklist for systems under the control and monitoring of watchkeeping engineers can prevent forced shutdowns related to the exhaust system, particularly through regular monitoring of exhaust temperatures.

Monthly oil analysis (particulate matter/viscosity/BN) results in the lubrication system should be visualized using a "traffic light" approach. Laboratory results should be closely monitored by the office and the ship. Onboard oil analyses should be increased in frequency, and all engineers should be trained on this subject.

To support these systems, which frequently cause shutdowns, the minimum critical onboard inventory (fuel valve nozzles, plunger/barrel, exhaust valve spares, pressure/temperature sensors, filters) should be recalculated according to route and lead time; low-threshold warnings should be entered into the planned maintenance system. The goal is to reduce the number of stoppages caused by these three by ≥15% per year and to shorten the wait per event by ≥30 min.

Delays in OMD-related shutdowns often arise from the inability to quickly distinguish between true and false alarms. A three-tiered approach is recommended for every ship: (i) Hardware: Sensor calibration intervals should be shortened; a 2-minute quick checklist for aspiration lines, filters, and sampling should be standardized. (ii) Workflow: A one-page "procedure/verification protocol" (reserve sensor, local heat/vibration, oil mist monitoring) to be followed when an alarm occurs should be visible in the engine control room. (iii) Recording: The "alarm time-verification steps-result" fields should be mandatory in the engine room logbook. The goal is to reduce unnecessary OMD-related delays by 30% and reduce verification time in real-world situations to <5 minutes.

The utility of the CART decision tree depends on up-to-date and consistent data. Mandatory, coded fields (system/subsystem, start and end, steps implemented, verification period, result) should be added to incident forms; free text should be kept to a minimum. The model should be retrained at least annually with new data; tree depth, number of terminal nodes, R^2, and RMSE should be reported. The risk thresholds used in Pareto should be updated with annual reviews based on fleet age, fuel quality, or line changes. A "top three root causes - top three actions" table should be communicated to the fleet through ship-to-office feedback meetings. Average waiting per stop, incident frequency, and duration in critical clusters should be monitored as indicators of success.

To translate technical measures into lasting results, a structured fleet-wide competency development program is recommended. A role-based competency matrix (3rd, 2nd, chief engineer, electrician, etc.) should be established. OMD alarm management, critical subsystem diagnostics derived from CART, fuel-exhaust-lubrication package procedures, and shaft line early warning signals should be core modules within this matrix.

Two channels for training delivery: (i) Microlearning (10-12-minute videos/notes), (ii) scenario-based exercises (monthly online + quarterly live demonstration). Standardized checklists and time objectives should be used for each scenario. An onboarding package, familiarization training (first 30 days) should be mandatory for newly appointed personnel, and competency should be verified with an annual refresher exam (≥80% success). To track the impact of training, KPIs (Key Performance Indicators) (training participation rate, drill success score, and fault response time after training) should be monitored, and ships with low performance should be inspected and trained. The goal is to reduce downtime in critical clusters by 10-15% and diagnosis times by 20% in the first 12 months after training.

6. Conclusion

This study presents a fleet-scale analysis of unscheduled downtime in container ship operations based on five years of operational records from 50 vessels. By combining risk-based Pareto analysis with an interpretable CART regression framework, the research identifies a limited number of technical subsystems that dominate both downtime frequency and duration. The results demonstrate that propulsion-related failures particularly those associated with the main engine fuel, exhaust, lubrication, and oil mist detection systems account for a disproportionate share of operational disruption, despite the presence of numerous lower-impact failure modes.

Beyond identifying critical failure clusters, the study contributes a practical, data-driven framework that links empirical downtime patterns to maintenance prioritization and role-based training strategies. The emphasis on interpretability enables direct translation of analytical outcomes into actionable decisions for fleet managers and marine engineers. While the findings are specific to container ship operations within a homogeneous fleet, the proposed analytical approach is transferable to other vessel types and operational contexts. Future studies may extend this framework by incorporating additional fleets, integrating exposure-normalized indicators, and evaluating long-term performance improvements resulting from targeted maintenance and training interventions.

Footnote

Financial Disclosure: The author declared that this study received no financial support.

References

[1] A. S. Kalafatelis, N. Nomikos, A. Giannopoulos, G. Alexandridis, A. Karditsa, and P. Trakadas, “Towards predictive maintenance in the maritime ındustry: a component-based overview,” *Journal of Marine Science and Engineering,* vol. 13, no. 3, 425, Feb 2025,

[2] D. Budimir, D. Medić, V. Ružić, and M. Kulej, “Integrated approach to marine engine maintenance optimization: Weibull Analysis, Markov Chains, and DEA model,” *Journal of Marine Science and Engineering,* vol. 13, no. 4, 798, Apr 2025.

[3] T. Tinga, W. Tiddens, F. Amoiralis, and M. Politis, “Predictive maintenance of maritime systems: models and challenges,” in *Safety and Reliability – Theory and Applications*, High Tatras Mountains, Tatranské Matliare, Slovak Republic: CRC Press, June 2017, pp. 68.

[4] H. Shen, H. Cao, L. Wang, Z. Ai, and S. Dai, “Multi-granularity graph reasoning for semantic entity recognition in maritime fault knowledge extraction,” *Knowledge-Based Systems,* vol. 328, 114170, Oct 2025.

[5] J. Karmelić, M. Jović Mihanović, A. Perić Hadžić, and D. Brčić, “Liner schedule reliability problem: an empirical analysis of disruptions and recovery measures in container shipping,” *Logistics*, vol. 9, no. 4, 149, Oct 2025.

[6] V. H. Nguyen, “Optimal ship maintenance scheduling under restricted conditions and constrained resources,” *Old Dominion University Libraries,* 2017.

[7] R. Islam, F. Khan, R. Abbassi, and V. Garaniya, “Human error assessment during maintenance operations of marine systems – What are the effective environmental factors?,” *Safety Science*, vol. 107, pp. 85-98, Aug 2018.

[8] K. Ünlügençoğlu, “An investigation of maritime accidents in Turkish territorial waters,” *Journal of Naval Architecture and Marine Technology,* vol. 2024, no. 226, pp. 65-79, Jan 2025.

[9] E. Romano-Moreno, G. Diaz-Hernandez, A. Tomás, and J. L. Lara, “Multivariate assessment of port operability and downtime based on the wave-induced response of moored ships at berths,” *Ocean Engineering*, vol. 283, 115053, Sept 2023.

[10] L. M. Millefiori et al., “COVID-19 impact on global maritime mobility,” *Scientific Reports,* vol. 11, no. 1, 18039, Sep 2021.

[11] D. Simion, F. Postolache, B. Fleacă, and E. Fleacă, “AI-driven predictive maintenance in modern maritime transport—enhancing operational efficiency and reliability,” *Applied Sciences,* vol. 14, no. 20, 9439, Oct 2024.

[12] H. R. Soltani Motlagh, S. B. Issa-Zadeh, M. R. Zoolfakar, and C. L. Garay-Rondero, “Enhancing ship propulsion efficiency predictions with integrated physics and machine learning,” *Journal of Marine Science and Engineering,* vol. 13, no. 8, 1487, Jul 2025.

[13] V. J. Jimenez, N. Bouhmala, and A. H. Gausdal, “Developing a predictive maintenance model for vessel machinery,” *Journal of Ocean Engineering and Science*, vol. 5, no. 4, pp. 358-386, Dec 2020.

[14] A. BahooToroody, M. M. Abaei, E. Zio, F. Goerlandt, and M. Chaal, “Gaussian process latent variable model and Bayesian inference for non-parametric failure modeling applied to ship engine,” *Reliability Engineering and System Safety,* vol. 265, 111611, Jan 2026.

[15] D. E. Onwuegbuchunam, I. C. Ogwude, C. C. Igboanusi, K. O. Okeke, and N. N. Azian, “Propulsion shaft and gearbox failure in marine vessels: a duration model analysis,” *Journal of Transportation Technologies,* vol. 10, no. 04, pp. 291-305, Jan 2020.

[16] L. Chybowski, M. Szczepanek, K. Gawdzińska, and O. Klyus, “Particles morphology of mechanically generated oil mist mixtures of SAE 40 grade lubricating oil with diesel oil in the context of explosion risk in the crankcase of a marine engine,” *Energies*, vol. 16, no. 9, 3915, May 2023.

[17] V. S. Ivanov, S. M. Frolov, I. V. Semenov, and M. S. Belotserkovskaya, “Crankcase explosions in marine diesel engines: a computational study of unvented and vented explosions of lubricating oil mist,” *Journal of Marine Science and Engineering,* vol. 12, no. 1, p. 82, Dec 2023.

[18] B. O. Ceylan, and M. S. Celik, “Operational risk assessment of marine boiler plant for on-board systems safety,” *Applied Ocean Research,* vol. 144, 103914, Mar 2024.

[19] S. Ahmed and X.-C. Gu, "Accident-based FMECA study of marine boiler for risk prioritization using fuzzy expert system," *Results in Engineering*, vol. 6, 100123, Jun 2020,

[20] X. Xu, X. Yan, K. Yang, J. Zhao, C. Sheng, and C. Yuan, "Review of condition monitoring and fault diagnosis for marine power systems," *Transportation Safety and Environment,* vol. 3, no. 2, pp. 85-102, Jun 2021.

[21] M. Tekgoz, Y. Garbatov, and C. Guedes Soares, "Strength assessment of an intact and damaged container ship subjected to asymmetrical bending loadings," *Marine Structures,* vol. 58, pp. 172-198, Mar 2018.

[22] O. Gaidai, F. Wang, Y. Cao, and Z. Liu, "4400 TEU cargo ship dynamic analysis by Gaidai reliability method," *Journal of Shipping and Trade,* vol. 9, no. 1, p. 1, Jan 2024.

[23] X. Zhang, and S. Mahadevan, "Bayesian network modeling of accident investigation reports for aviation safety assessment," *Reliability Engineering & System Safety,* vol. 209, 107371, May 2021.

[24] J. Yu, J. Zhao, X. Wang, and Y. Cao, "Maritime occupational accidents analysis: a data-driven Bayesian network approach," *Ocean Ocean & Coastal Management,* vol. 269, 107785, Oct 2025.

[25] L. Breiman, J. Friedman, C. J. Stone, and R. A. Olshen, *Classification and regression trees (CART)*. Taylor & Francis, 1984. [Online]. Available: https://books.google.com.tr/books?id=JwQx-WOmSyQC

[26] G. Vizentin, G. Vukelic, L. Murawski, N. Recho, and J. Orovic, "Marine propulsion system failures—a review," *Journal of Marine Science and Engineering*, vol. 8, no. 9, p. 662, Aug 2020.

[27] R. Kuroiwa, T. Nishioka, A. Oshima, K. Ohyama, T. Tateishi, and T. Ishijima, "*Reliability ımprovement of stern tube bearing considering propeller shaft forces during ship turning* (Mitsubishi Heavy Industries, Ltd. Technical Review, vol. 44, no. 3)," Mitsubishi Heavy Industries, Ltd. Technical Review, 2007.

[28] X. Chang, J. Liu, X. Yan, F. Sun, H. Zhu, and C. Wang, "Experimental study on the effects of controllable parameters on the healthy operation of SF-2A material water-lubricated stern bearing in multi-point ultra-long shaft systems of ships," *Journal of Marine Science and Engineering*, vol. 13, no. 1, p. 14, Dec 2024.

[29] A. Thorpe and S. Pabby, "Effectiveness of oil mist detectors in relation to oil mist droplet size and concentration," Symposium Series no. 162, 2017.

RESEARCH ARTICLE
DOI: 10.4274/jems.2025.27167
J Nav Architect Mar Technol 2026;228:24-31

An Investigation on the Effects of Different Solvents on the Characteristics of a Carbon Capture System in a Tanker

Furkan Böbür[1], Engin Güler[1,2], Selma Ergin[1]

[1]İstanbul Technical University Faculty of Naval Architecture and Ocean Engineering, Department of Naval Architecture and Marine Engineering, İstanbul, Türkiye
[2]Piri Reis University Faculty of Engineering, Department of Naval Architecture and Marine Engineering, İstanbul, Türkiye

To cite this article: F. Böbür, E. Güler, and S. Ergin. An investigation on the effects of different solvents on the characteristics of a carbon capture system in a tanker. *J Nav Architect Mar Technol*. 2026;228:24-31.

Received: 28.09.2025 - **Revision Requested:** 21.11.2025 - **Last Revision Received:** 22.12.2025 - **Accepted:** 21.01.2026 - **Publication Date:** 04.02.2026

Abstract

Harmful emissions into the atmosphere, such as carbon dioxide (CO_2), are increasing due to the extremely use of fossil fuels in the world. The shipping also increases global CO_2 emissions. This results in critical ecological issues like global warming, climate change and air pollution. Therefore, applications to reduce CO_2 emissions are needed, and carbon capture is one of these. In this study, the effects of mono-ethanolamine (MEA), piperazine (PZ) and ammonia (NH_3) solvents on the carbon capture costs and CO_2 capture rates (%) of the carbon capture system aboard a tanker were investigated for 30 wt% solvents. Capturing performance and economic analyses of the carbon capture system aboard the 49.990 DWT tanker were performed using Aspen HYSYS software. For different solvents, annual captured CO_2 emission amounts and CO_2 capture rates (%) were obtained at 85% engine load-cruise mode. For the same geometries of carbon capture columns, the carbon capture costs of the system per ton of CO_2 are \$82.6, \$69.6, and \$47.3 for MEA, PZ and NH_3 solvents, respectively and the CO_2 capture rates are 30.9%, 36.7%, and 54% for MEA, PZ and NH_3 solvents, respectively. Cost-effective capture of CO_2 emissions released from ships into the atmosphere is important for the widespread use of carbon capture and storage systems.

Keywords: Carbon capture and storage, decarbonization, CO_2 emission, tanker, solvent

1. Introduction

Harmful emissions emitted into the atmosphere by usage of fossil fuels are increasing because of increasing energy need for various industries and home usage. Approximately 87% of carbon dioxide (CO_2) production resulting from human activities is the result of burning fossil fuels [1]. Thus, this causes adverse consequences like global warming, climate change, and air pollution. The shipping sector has a share of over 80% of the goods transported by volume on global trade. Also, its proportion of greenhouse gas (GHG) emission to global GHG emission is approximately 3% [2]. GHG emissions from ships are going up due to the increasing dimensions of ships and fleets even though GHG emissions by maritime industry have small share among other transportation modes and industries. Some regulations, such as the Ship Energy Efficiency Management Plan (SEEMP) and the Energy Efficiency Design Index (EEDI) were launched in amendments to *International Convention for the Prevention of Pollution from Ships*-MARPOL Annex VI by the International Maritime Organization (IMO) [3]. The target of the EEDI is to make ships energy-efficient in the

Address for Correspondence: Prof. Selma Ergin, İstanbul Technical University Faculty of Naval Architecture and Ocean Engineering, Department of Naval Architecture and Marine Engineering, İstanbul, Türkiye
E-mail: ergin@itu.edu.tr
ORCID ID: orcid.org/0000-0001-8343-2455

design phase by optimizing their hull form and decreasing electric consumption by operational measures. The SEEMP aims to improve ships' energy efficiency and optimize the operational performance of ships by operational adjustments, such as installing waste heat recovery (WHR) equipment, optimizing the speed of ships, and weather routing. Also, the SEEMP is obligatory for ships above 400 gross tonnages [3]. The Energy Efficiency Existing Ship Index (EEXI) is another regulation by the IMO about enhancement of ships' energy efficiency. The target of the EEXI is to enhance the energy efficiency of ships already in operation and decrease GHG emissions from shipping [4]. The Carbon Intensity Indicator (CII) is another regulation by the IMO regarding the evaluation of GHG emissions on the volume of loads and miles transported. Also, the required annual reduction factor to be met by a ship on her operations is determined by the CII and the efficiency categories are A, B, C, D, and E for a ship [5]. The Monitoring, Reporting and Verification system is a regulation by the European Union (EU) to assess CO_2 emissions from ships by monitoring and reporting fuel consumption and CO_2 emissions of ships per voyage and on yearly basis, based on ships above 5000 gross tonnes at European Economic Area (EEA) ports. Companies from shipping industry must submit a monitoring plan for each ship and the data collected must be verified by accredited third parties [6]. This regulation is significant to increase the transparency and awareness of GHG emissions from shipping for decreasing fuel consumption and emissions. The IMO aims to reach a 20% reduction by 2030 and a 70% reduction by 2040 in GHG emissions, compared to 2008 level. Also, IMO aims to have net zero emissions by 2050 [7]. Moreover, the EU has target to decrease GHG emissions by 55%, based on the 1990 level, by 2030. This is evaluated economically feasible and beneficial by the EU [8]. Therefore, decarbonization of ships and carbon capture and storage (CCS) have become significant working fields to be considered [9].

There are many studies regarding CCS in the literature. Van Duc Long et al. [10] conducted a marine CO_2 capture study on a 3000-kW diesel engine with different configurations to evaluate CO_2 removal performance of the systems. Mono-ethanolamine (MEA), MEA/piperazine, (MEA/PZ) and n-methyl-diethanolamine/PZ are considered as solvents in this study. The results revealed that the CO_2 removal performance of proposed configuration was obtained as 94.7% and there is an increase of 8.4% in comparison with the base case. Tavakoli et al. [11] studied about the feasibility of carbon capture onboard ships. Retrofit and newbuild ships are considered for assessment the technical feasibility using the solvent-based post-combustion capture in this study. The results indicated that limited space and additional power required are challenges for the retrofit case. Also, it is challenging to find adequate space for CO_2 storage in terms of cargo capacity. Brandl et al. [12] conducted a study to obtain the hypothetical solvent to achieve the cost reduction by comparing the performances of various solvents. The results showed that a 65% of cost reduction was achieved and a cost limit of \$26/ton CO_2 (\$: US Dollars, weight unit: ton) was obtained. Zhou et al. [13] conducted a study on the carbon capture specifications of the exhaust gas of a marine engine. In this study, a K_2CO_3 solution was used in the simulation of CO_2 capture from the exhaust gas using ASPEN Plus. Various activators used in the experiment were selected using simulation results. The results showed that the absorption rate of CO_2 from the exhaust gas of the marine engine can be improved by a small amount of activator. Mao et al. [14] conducted a study on a mixed absorbent on the marine carbon capture. The characteristics of absorption and desorption were evaluated for different mole ratios. The results indicated that the average CO_2 absorption rate increased by 48% in comparison with MEA. Güler and Ergin [15] conducted a study on a solvent-based CCS system. Various types of ships are considered to investigate the performance of a system and to analyze its cost for different ships in this study. The results showed that the CCS system is more economic than other CO_2 control methods for ships with high speed. Bayramoğlu [16] conducted a study about post-combustion carbon capture on a marine engine. WHR and carbon capture system are considered to examine the rate of carbon reduction and the EEDI for ships. In this system, there is a 14% reduction of EEDI by WHR, and by 90% with the carbon capture. The results indicated that the carbon capture can be a promising method to meet the regulations.

There is no such study has investigated the effects of various solvents on capturing and economic performance of a solvent-based CCS system aboard a tanker by considering the actual general arrangement of a ship in the literature. Available space of the general arrangement of the ship is evaluated for the system because there is limited space for the columns of the system onboard the ship. The aim of this study is to investigate the effects of various solvents on the annual amount of the CO_2 emission captured and CO_2 capture rate (%) at the engine load of 85%, cruising mode. The other objective is to compute the carbon capture cost of the system per ton of CO_2 captured for different solvents. A 49,990-DWT tanker was examined in this study. MEA, PZ and, ammonia (NH_3) were considered as solvents.

2. Mathematical Model of CCS System

2.1. Carbon Capturing Model

Capturing performance analysis of the solvent-based CCS system aboard a tanker is conducted by using ASPEN software. The CCS system is modeled. MEA, PZ and, NH_3 are considered as solvents in this study. MEA is a common solvent and its some advantages are low volatility and relatively fast kinetics. However, its some disadvantages are high oxidative degradation and relatively high energy demand [17]. PZ has fast kinetics and low degradation rate [10]. Also, it has high thermal stability and less volatility in comparison with conventional amine-based alkanolamine [18]. NH_3 has a lower heat of reaction for absorption of CO_2 compared to MEA and the disadvantage of NH_3 is its volatility [19]. Furthermore, NH_3 is highly corrosive, and metal materials should be protected from contact with it. NH_3 is a toxic substance, and prolonged exposure to it should be avoided for health reasons. Additionally, fast kinetics, less tendency to degradation, less corrosive and less toxicity are some of the criterion on solvent selection for solvent-based CCS system [20]. In the process of absorption of CO_2 by the MEA solution, following chemical reactions take place, as shown in Equations (1-5) [15]:

$$MEACOO^- + H_2O \leftrightarrow MEA + HCO_3^- \tag{1}$$

$$CO_2 + 2H_2O \leftrightarrow HCO_3^- + H_3O^+ \tag{2}$$

$$HCO_3^- + H_2O \leftrightarrow CO_3^{-2} + H_3O^+ \tag{3}$$

$$MEAH^+ + H_2O \leftrightarrow MEA + H_3O^+ \tag{4}$$

$$2H_2O \leftrightarrow H_3O^+ + OH^- \tag{5}$$

MEA solution is a benchmark to compare capturing performance due to its reaction rate [10]. In absorption of CO_2 by the PZ solution, following reactions occur, as shown in Equations (6-10) [18]:

$$H_2O \leftrightarrow H^+ + OH^- \tag{6}$$

$$PZH^+ \leftrightarrow PZ + H^+ \tag{7}$$

$$PZ + CO_2 \leftrightarrow PZCOO^- + H^+ \tag{8}$$

$$PZCOO^- + CO_2 \leftrightarrow PZ(COO^-)_2 + H^+ \tag{9}$$

$$H^+PZCOO^- \leftrightarrow PZCOO^- + H^+ \tag{10}$$

Chemical equilibrium constants for the PZ solution reactions are calculated [18]. For NH_3, following reactions occur, as shown in Equations (11, 12) [19]:

$$CO_2 + OH^- \leftrightarrow HCO_3^- \tag{11}$$

$$NH_3 + CO_2 + H_2O \leftrightarrow NH_2COO^- + H_3O^+ \tag{12}$$

Chemical equilibrium constants for the NH_3 solution reactions are calculated [19]. The annual amount of the CO_2 emissions emitted from the ship into the atmosphere and CO_2 capture rate (%) are required to compute the annual amount of the CO_2 captured by the system. The annual amount of the CO_2 emission emitted from the ship [t] is computed by using specific fuel oil consumption (SFOC) [g/kWh], power [kW], emission factor (EF), and annual operational time [h] of the main engine, as shown in Equation (13).

$$\text{Annual } CO_2 \text{ emission=SFOC*Power*Annual operational time*EF} \tag{13}$$

CO_2 capture rate (%) is the ratio of the CO_2 transferred from the stripper to CO_2 storage onboard to captured CO_2 by the absorber. The annual amount of the CO_2 captured by the system is calculated by using the annual amount of the CO_2 emission emitted from the ship into the atmosphere and CO_2 capture rate (%), as shown in Equation (14).

$$\text{Annual } CO_2 \text{ captured=Annual } CO_2 \text{ emission*} CO_2 \text{ capture rate} \tag{14}$$

2.2. Economic Model

The carbon capture cost of the system per ton of CO_2 captured (C_{PCC}) was obtained for different solvents in economic analysis. The equipment and its installation cost (C_{EI}) and the other capital cost (C_O), such as engineering services and commissioning, are calculated using ASPEN software. The total capital cost (C_T) is calculated by the sum of the equipment and its installation cost (C_{EI}) and the other capital cost (C_O), as shown in Equation (15).

$$C_T = C_{EI} + C_O \tag{15}$$

The annualized total capital cost (C_{AT}) is computed by using C_T and the capital recovery factor (CRF), as shown in Equations (16, 17). The life of a ship is assumed as 25 years (n) and interest rate (i) is assumed as 10% without inflation [21].

$$CRF = \frac{i(1+i)^n}{(1+i)^n - 1} \tag{16}$$

$$C_{AT} = C_T CRF \tag{17}$$

The annual operational cost (C_{AO}) is calculated by using the freight loss cost (C_{FL}) due to the weight of the CCS system and additional fuel consumption cost (C_{AFC}) due to the additional power need for the system, as shown in Equation (18).

$$C_{AO} = C_{FL} + C_{AFC} \tag{18}$$

The annual life cycle cost (C_{ALC}) is calculated by using the annualized total capital cost (C_{AT}) and the annual operational cost (C_{AO}), as shown in Equation (19).

$$C_{ALC} = C_{AT} + C_{AO} \tag{19}$$

C_{PCC} is the ratio of the annual life cycle cost (C_{ALC}) to the CO_2 captured annually (T_{CCA}), as shown in Equation (20).

$$C_{PCC} = \frac{C_{ALC}}{T_{CCA}} \tag{20}$$

3. Specification of The Tanker, Selected Solvents and The CCS System

3.1. Specification of the Tanker

In this study, the ship considered and her properties of the diesel main engine at various engine loads are given in Tables 1 and 2.

EFs for a slow-speed marine diesel engine are used in this study. EFs are 3170 kg/ton of fuel for CO_2, 7.4 kg/ton of fuel for CO, 87 kg/ton of fuel for NO_X and 54 kg/ton of fuel for SO_2 [22].

3.2. Properties of Selected Solvents

In this study, MEA, PZ and, NH_3 are considered as solvents. MEA's chemical formula is C_2H_7NO and its molecular weight is 61.1 g. Its density at 20 °C is 1016 kg/m^3, and its melting and boiling points are 4 and 167 °C, respectively [23]. PZ's chemical formula is $C_4H_{10}N_2$ and its molecular weight is 86.1 g. Its density at 50 °C is 1020 kg/m^3, and its melting and boiling points are 35-45 and 110 °C, respectively [23]. NH_3's chemical formula is NH_3 and its molecular weight is 17 g. Its density at 15 °C is 0.73 kg/m^3, and its melting and boiling points are -77.7 and -33.3 °C, respectively.

Table 1. The particulars of the ship [22].

Features	Value
Length overall	183 m
Beam	32.2 m
Draft	16.5 m
Deadweight	49,990 t
Installed power (main engine)	10,320 kW

3.3. Properties of the CCS System

In the CCS system, the CO_2 emissions from the exhaust gas of the main engine is captured in the absorber. The CO_2-rich solvent is directed to pump to transfer to heat exchanger, whereas the clean gas from the residual exhaust gas is released. CO_2-solvent mixture is directed to stripper after heating by the heat exchanger. CO_2 is separated from the mixture in the form of gas in the stripper by heating and transferred to the CO_2 storage tank on-board and liquefied. CO_2-solvent mixture without CO_2 is cooled by the heat exchanger to re-use and directed to absorber, as shown in Figure 1.

Additional power is required for CCS due to processes such as, heating, cooling, pumping, and liquefaction. Also, extra space is needed for CO_2 storage in ships. The dimensions of the absorber and the stripper, and the power of the heat exchanger, and the pump are significant on carbon capture rate, the cost per ton of CO_2 captured, and occupied area on a ship. CCS system has also effects on the stability of ships because of its extra weight, area and location at a ship and freight revenue because of decreasing the amount of goods transported. The main aim of the carbon capture systems is contributing to cleaner and more sustainable environment based on regulations regarding reduction in GHG emissions. The optimization of the cost and dimensions of these systems are important to use widely on ships. In this study, MEA, PZ and, NH_3 are considered as solvents. The carbon capture system is located at the near of the funnel of the ship [24].

Table 2. The properties of the main engine at various engine loads [22].

Load (% Maximum continuous rating)	Power (kW)	SFOC (g/kWh)	Exhaust gas mass flow rate (kg/s)	Exhaust gas temperature (°C)
100	10,320	176.4	23.4	255
95	9,804	175.1	22.4	248
90	9,288	174.1	21.7	243
85	8,772	173.3	20.9	239
80	8,256	172.7	20.1	236
75	7,740	172.3	19.1	235
70	7,224	172.2	18.2	235
65	6,708	172.5	17.1	237
60	6,192	173.0	16.1	240
55	5,676	173.9	14.9	244
50	5,160	174.8	13.8	250

SFOC: Specific fuel oil consumption

4. Results and Discussion

4.1. Capturing Performance Analysis

Capturing performance analysis is carried out by using ASPEN HYSYS package program in this study. Firstly, solvents and fluids considered in this study are selected in the component list. Then, the solution method is selected. Acid gas-chemical solvents package is used in this study. Additionally, acid gas-chemical solvents package is a method, which is developed with the Peng-Robinson equation of state for vapor phase. Afterwards, the components in this system are selected and the system is formed. Conditions, such as temperature, pressure, and mass flow rate, are determined in this system. Lastly, CO_2 capture rates are obtained for MEA, PZ, and NH_3 at the engine load of 85%, cruising mode. The temperature of 30 °C and the pressure of 102 kPa are used for all solvents in this study. The volumetric flow rates of these solvents are 150, 168 and 248 m^3/h for MEA, PZ, and NH_3 solvents, respectively. The diameter and height of the absorber and stripper columns, space available on the ship for the CCS system, annual operational time of the main engine of the ship, and CO_2 EF (g-CO_2/kWh) of the marine main engine are some key parameters in capturing performance analysis. In this study, the absorber and stripper columns' diameters are equal and 1.5 m according to the general arrangement of the tanker. Both absorber and stripper have 10 stages. Also, they are tray columns and tray spaces are 0.6 m. Mass transfer in these columns are computed using the mass, equilibrium, summation of vapor and liquid compositions and heat (MESH) equations by Aspen HYSYS software based on the equilibrium-based model [18]. Additionally, the composition of exhaust gas is modelled as nitrogen of 67%, CO_2 of 12%, water of 11%, and oxygen of 10% by weight, respectively [25]. The annual amount of the CO_2 emission emitted from the ship into the atmosphere at the engine load of 85%, cruising mode, for a duration of 6400 hours of operational time is calculated as 30,842 tons of CO_2. CO_2 capture rates are calculated as 30.9%, 36.7% and 54% for MEA, PZ and NH_3 solvents, respectively. Also, the annual amounts of CO_2 captured are obtained as 9,530 tons, 11,319 tons and 16,655 tons for MEA, PZ and NH_3 solvents, respectively. Annual CO_2 captured is maximum for NH_3 solvent because of higher CO_2 capture rate of NH_3 solvent compared to other solvents in this study, as shown in Figure 2.

4.2. Economic Analysis

Economic analysis is conducted for MEA, PZ and, NH_3 30 wt% (wt: percentage by weight) at the engine load of 85%, cruising mode. In the scope of this analysis, the carbon capture cost of the system per ton of CO_2 (C_{PCC}) is calculated using the system annual life cycle cost and the annual amount of the CO_2 captured by the system. The cost of the system consists of equipment, construction, buildings, engineering and supervision costs [26]. In this analysis, the share of this types of costs are 50.5%, 29%, 4.7% and 15.8%, respectively. The equipment and its installation cost (C_{EI}) is calculated as \$2,001,330 and the other capital cost (C_O) is \$516,067. The total capital cost (C_T) is \$2,517,397 and the CRF is calculated as 0.11 for the life of a ship of 25 years (n) and interest rate (i) of 10% without inflation. The annualized total capital cost (C_{AT}) is \$277,342. Also, the annual operational cost (C_{AO})

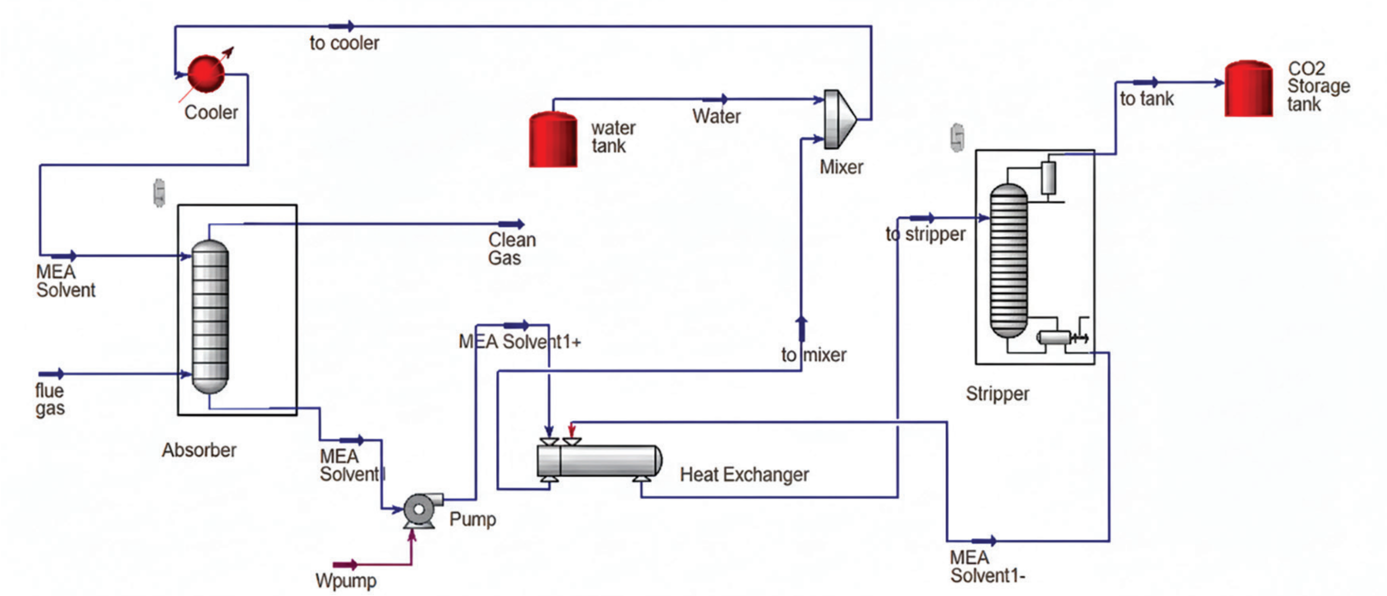

Figure 1. Schematic of CCS system considered in this study.

CCS: Carbon capture and storage, CO_2: Carbon dioxide, MEA: Mono-ethanolamine

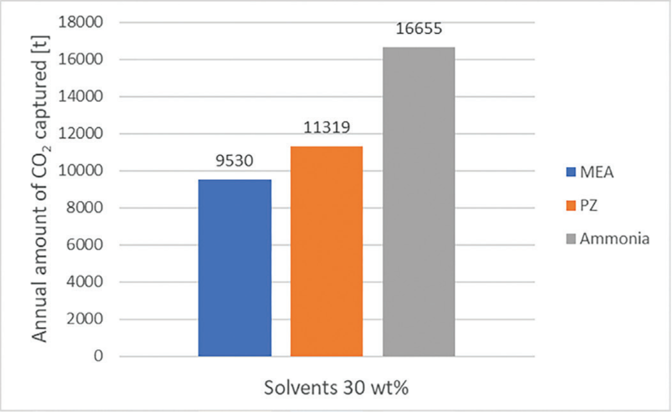

Figure 2. Relation between solvents and annual CO_2 captured by the CCS system.

CCS: Carbon capture and storage, MEA: Mono-ethanolamine, CO_2: Carbon dioxide, PZ: Piperazine

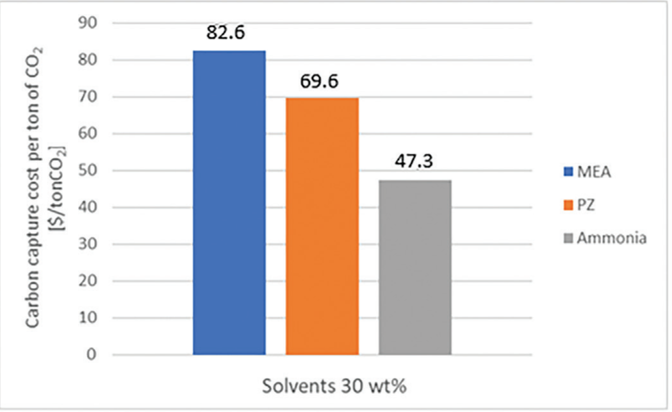

Figure 3. Relation between solvents and C_{PCC} of the CCS system.

CCS: Carbon capture and storage, MEA: Mono-ethanolamine, PZ: Piperazine

is calculated as $510,159 with the assumption of additional fuel consumption cost of the system for capturing the CO_2 emissions as 5% of the fuel consumption of the ship and freight loss cost as 10% of the sum of the equipment and its installation cost (C_{EI}) and the buildings cost [18]. Also, the annual life cycle cost (C_{ALC}) is calculated as $787,501, as shown in Table 3.

C_{PCC} is $82.6 for MEA solvent for the CO_2 capture rate of 30.9%, $69.6 for PZ solvent for the CO_2 capture rate of 36.7% and $47.3 for NH_3 solvent for the CO_2 capture rate of 54%, as shown in Figure 3.

C_{PCC} is minimum for NH_3 solvent because of higher annual CO_2 captured for NH_3 solvent compared to other solvents in this study. Moreover, the EU Emission Trading System (ETS) is a regulation set by the EU. With the ETS, ships pay for their emissions emitted into the atmosphere and the price is determined by the EU using the value of the amount of annual emission from ships and the EU ETS prices are shown in Figure 4.

Table 3. Cost components of the CCS system.

Features	Values
C_{EI}	$2,001,330
C_O	$516,067
C_T	$2,517,397
C_{AT}	$277,342
C_{AO}	$510,159
C_{ALC}	$787,501
CRF	0.11
n	25 years
i	10%

CCS: Carbon capture and storage, CRF: Capital recovery factor

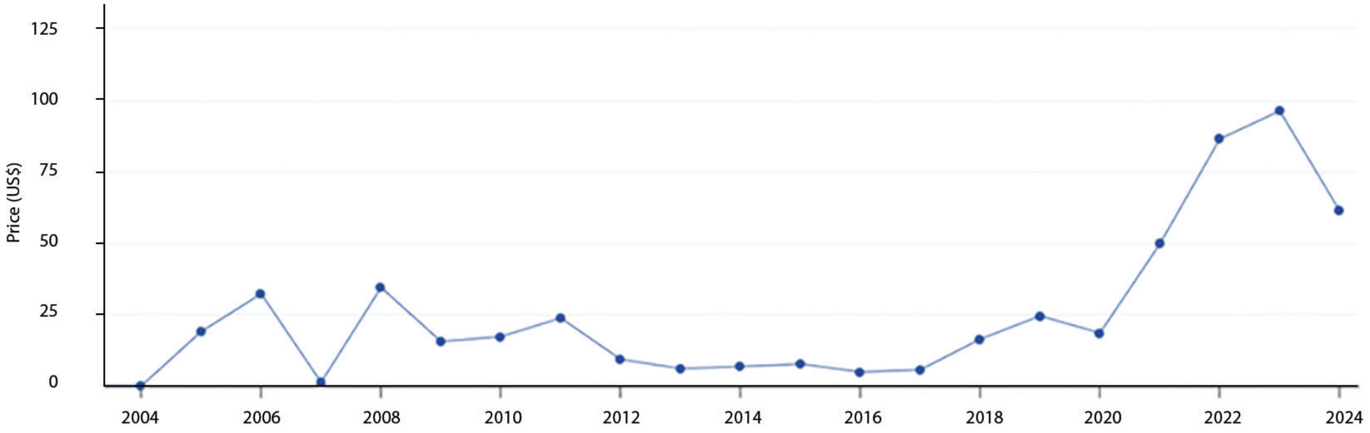

Figure 4. Trends in EU ETS between 2004 and 2024 [$/tonCO$_2$] [27].

EU: European Union, ETS: Emission Trading System

C_{PCC} for MEA and PZ in this study is higher than the EU ETS price in 2024. However, the cost for NH_3 is less than the EU ETS price in 2024. According to the new EU ETS II, carbon prices (in European Currency Unit) can go up €122/tCO_2 (\$144/tCO_2) in 2030 and a mean of €99/tCO_2 at the period of 2027 and 2030 [28]. In the near future, this technology can be considered economically feasible with increasing ETS prices and decreased C_{PCC} for ships. When C_{PCC} is higher than ETS and/or carbon tax, this is a barrier for these systems to be feasible for ship owners. Therefore, studies for the reduction of C_{PCC} are important for cleaner and sustainable shipping. Economic results from this study and the literature are given in Table 4.

Table 4. Economic results from this study and the literature.

Carbon capture cost (\$/tonCO_2)	References
149 (capture rate of 60%) 117 (capture rate of 90%)	[17]
70.34 (capture rate of 91%)	[29]
65.35 (capture rate of 34.5%)	[15]
77.50 (capture rate of 73%)	[21]
389 (capture rate of 60%) 296 (capture rate of 80%)	[30]
82.6 (capture rate of 30.9%) 69.6 (capture rate of 36.7%) 47.3 (capture rate of 54%)	From this study

According to Table 4, most of C_{PCC} from different studies are higher than the EU ETS prices. Therefore, the results in this study are consistent with various studies in the literature. Cost-effective reduction of CO_2 emissions released from ships into the atmosphere is important for the widespread use of carbon capture systems. Also, CCS on ships are important to reduce the adverse effects of the emissions of ships to the environment and human health.

5. Conclusion

The effects of MEA, PZ and NH_3 solvents on the carbon capture costs and CO_2 capture rates of the carbon capture system aboard a tanker were investigated for 30 wt% solvents in this study. Capturing performance and economic analyses of the CCS system aboard the 49.990 DWT tanker were performed using ASPEN HYSYS software. For different solvents, annual CO_2 emission amounts and CO_2 capture rates (%) were obtained at 85% engine load-cruise mode. The annual amount of the CO_2 emission emitted from the ship into the atmosphere at the engine load of 85%, cruising mode, for a duration of 6400 hours of operational time is calculated as 30,842 tons of CO_2. For MEA solvent 30 wt%, CO_2 capture rate is calculated 30.9% and the annual amount of CO_2 captured is 9,530 tons. Also, C_{PCC} is \$82.6 for MEA solvent 30 wt%. C_{PCC} is \$69.6 for PZ solvent 30 wt% for the CO_2 capture rate of 36.7% and the annual amount of CO_2 captured is 11,319 tons. Also, C_{PCC} is \$47.3 for NH_3 solvent 30 wt% for the CO_2 capture rate of 54% and the annual amount of CO_2 captured is 16,655 tons. C_{PCC} in this study for MEA and PZ is higher than the EU ETS price in 2024. Whereas, the cost for NH_3 is less than the EU ETS price in 2024. This technology can be considered economically feasible with increasing ETS prices and decreased carbon capture cost per ton of CO_2 captured for ships. CCS on ships are important to reduce the adverse effects of the emissions of ships to the environment and human health in order to have cleaner and sustainable shipping industry based on the IMO's net zero emissions target by 2050.

Acknowledgements

The authors thank the Turkish Scientific and Technological Research Council of Türkiye, TÜBİTAK (2224-A-1919B022507858) and Istanbul Technical University, BAP (FHD-2025-47373 and Project ID: 47929) for the financial support they received during their research.

Footnotes

Authorship Contributions

Concept: E. Güler, and S. Ergin, Design: F. Böbür, and E. Güler, Data Collection or Processing: F. Böbür, E. Güler, and S. Ergin, Analysis or Interpretation: F. Böbür, E. Güler, and S. Ergin, Literature Review: F. Böbür, E. Güler, and S. Ergin, Writing: F. Böbür, E. Güler, and S. Ergin.

Conflict of Interest: No conflict of interest was declared by the authors.

Financial Disclosure: The authors would like to thank İstanbul Technical University Scientific Research Projects Coordination Unit (BAP) for providing financial support to the project numbered 44432.

References

[1] T. Wilberforce, A. G. Olabi, E. T. Sayed, K. Elsaid, and M. A. Abdelkareem, "Progress in carbon capture technologies," *Science of the Total Environment*, vol. 761, 143203, Mar 2021.

[2] UNCTAD, "Review of maritime transport 2023." Accessed: Dec 12, 2024. [Online]. Available: https://unctad.org/system/files/official-document/rmt2023_en.pdf

[3] E. K. Hansen, H. B. Rasmussen, and M. Lützen, "Making shipping more carbon-friendly? Exploring ship energy efficiency management plans in legislation and practice," *Energy Research & Social Science*, vol. 65, 101459, Jul 2020.

[4] S. Lee, "Analysis of the effects of EEDI and EEXI implementation on CO_2 emissions reduction in ships," *Ocean Engineering*, vol. 295, 116877, Mar 2024.

[5] IMO, “IMO regulations to introduce carbon intensity measures enter into force on 1 November 2022.” Accessed: Dec 14, 2024. [Online]. Available: https://www.imo.org/en/MediaCentre/PressBriefings/pages/CII-and-EEXI-entry-into-force.aspx

[6] European Parliament, “Monitoring, reporting and verification of CO2 emissions from maritime transport.”, Accessed: Dec 14, 2024. [Online]. Available: https://www.europarl.europa.eu/thinktank/en/document/EPRS_BRI(2019)642224

[7] IMO, “2023 IMO Strategy on Reduction of GHG Emissions from Ships.” Accessed: Dec 14, 2024. [Online]. Available: https://www.imo.org/en/OurWork/Environment/Pages/2023-IMO-Strategy-on-Reduction-of-GHG-Emissions-from-Ships.aspx

[8] European Commission, “Stepping up Europe’s 2030 climate ambition.” Accessed: Dec 14, 2024. [Online]. Available: https://eur-lex.europa.eu/legal-content/EN/TXT/?uri=celex:52020DC0562

[9] G. Mallouppas, and E. A. Yfantis, “Decarbonization in shipping industry: a review of research, technology development, and innovation proposals,” *Journal of Marine Science and Engineering*, vol. 9, pp. 415, Apr 2021.

[10] N. Van Duc Long, et al. “Improvement of marine carbon capture onboard diesel fueled ships,” *Chemical Engineering and Processing-Process Intensification*, vol. 168, 108535, Nov 2021.

[11] S. Tavakoli, et al. “Exploring the technical feasibility of carbon capture onboard ships,” *Journal of Cleaner Production*, vol. 452, 142032, May 2024.

[12] P. Brandl, M. Bui, J. P. Hallett, and N. Mac Dowell, “A century of re-exploring CO_2 capture solvents,” *International Journal of Greenhouse Gas Control*, vol. 120, 103771, Oct 2022.

[13] S. Zhou, et al. “Experimental study on carbon capture characteristics of marine engine exhaust gas by activated potassium carbonate absorbent,” *Environmental Science and Pollution Research*, vol. 30, pp. 80416-80431, Jun 2023.

[14] X. Mao, H. Chen, Y. Wang, X. Zhu, and G. Yang, “Study on benzylamine (BZA) and aminoethylpiperazine (AEP) mixed absorbent on ship-based carbon capture,” *Molecules*, vol. 28, 2661, Mar 2023.

[15] E. Güler, and S. Ergin, “An investigation on the solvent based carbon capture and storage system by process modeling and comparisons with another carbon control methods for different ships,” *International Journal of Greenhouse Gas Control*, vol. 110, 103438, Sep 2021.

[16] K. Bayramoğlu, “Application of post-combustion carbon capture process in marine diesel engine,” *Energy Sources Part a Recovery Utilization and Environmental Effects*, vol. 45, pp. 10909-10925, Aug 2023.

[17] J. A. Ros, et al. “Advancements in ship-based carbon capture technology on board of LNG-fuelled ships,” *International Journal of Greenhouse Gas Control*, vol. 114, 103575, Feb 2022.

[18] E. Güler, and S. Ergin, “An investigation of the cooling, heating and power systems integration with carbon capture and storage for LNG carriers,” *Ships and Offshore Structures*, vol. 19, pp. 610-624, Mar 2023.

[19] A. Awoyomi, K. Patchigolla, and E. J. Anthony, “CO_2/SO_2 emission reduction in CO_2 shipping infrastructure,” *International Journal of Greenhouse Gas Control*, vol. 88, pp. 57-70, Sep 2019.

[20] C. Ji, S. Yuan, M. Huffman, M. M. El-Halwagi, and Q. Wang, “Post-combustion carbon capture for tank to propeller via process modeling and simulation,” *Journal of CO2 Utilization*, vol. 51, 101655, Sep 2021.

[21] X. Luo, and M. Wang, “Study of solvent-based carbon capture for cargo ships through process modelling and simulation,” *Applied Energy*, vol. 195, pp. 402-413, Jun 2017.

[22] M. Akman, and S. Ergin, “An investigation of marine waste heat recovery system based on organic Rankine cycle under various engine operating conditions,” *Proceedings of the Institution of Mechanical Engineers Part M Journal of Engineering for the Maritime Environment*, vol. 233, pp. 586-601, May 2018.

[23] Nouryon, “Product data sheet.” Accessed: Jan 2, 2025. [Online]. Available: https://www.nouryon.com/products/

[24] DNV, “The potential of onboard carbon capture in shipping.” Accessed: Dec. 15, 2024. [Online]. Available: https://www.dnv.com/maritime/publications/the-potential-of-onboard-carbon-capture-in-shipping-download/

[25] İ. A. Reşitoğlu, K. Altinişik, and A. Keskin, “The pollutant emissions from diesel-engine vehicles and exhaust aftertreatment systems,” *Clean Technologies and Environmental Policy*, vol. 17, pp. 15-27, Jun 2014.

[26] Chemical Engineering, “The chemical engineering plant cost index.” Accessed: Jan 14, 2025. [Online]. Available: https://www.chemengonline.com/pci-home

[27] World Bank Group, “State and trends of carbon pricing dashboard.” Accessed: Jan 3, 2025. [Online]. Available: https://carbonpricingdashboard.worldbank.org/compliance/price

[28] BloombergNEF, Bloomberg Philanthropies, and European Climate Foundation, “EU ETS II pricing scenarios: balancing cuts and costs.” Accessed: Sep 22, 2025. [Online]. Available: https://assets.bbhub.io/promo/sites/16/EU_ETS_II_Pricing_Scenarios_Balancing_Cuts_and_Costs.pdf

[29] F. Zea, D. Tinoco, and C. Varela, “A techno-economic evaluation of post-combustion carbon capture using renewable ammonia with different process configurations,” *Case Studies in Chemical and Environmental Engineering*, vol. 8, 100502, Dec 2023.

[30] M. Feenstra, J. Monteiro, J. T. Van Den Akker, M. R. Abu-Zahra, E. Gilling, and E. Goetheer, “Ship-based carbon capture onboard of diesel or LNG-fuelled ships,” *International Journal of Greenhouse Gas Control*, vol. 85, pp. 1-10, Jun 2019.